City, University of London Institutional Repository

Fiber Optic Sensor Designs and Luminescence-based Methods for the detection of Oxygen and pH measurement

Jan Werner[123]*, Mathias Belz[2], Karl-Friedrich Klein[3], Tong Sun[1] and K.T.V. Grattan[1]

[1] School of Mathematics, Computer Science and Engineering, City, University of London, Northampton Square, EC1V 0HB, London, U.K.

[2] World Precision Instruments Germany GmbH, Pfingstweide 16, 61169 Friedberg, Germany

[3] THM, University of Applied Science, Wilhelm-Leuschner-Strasse 13, 61169 Friedberg, Germany

* Correspondence: jan.werner@city.ac.uk

Abstract: Optical, and especially fiber optic techniques for chemical sensing have become very attractive in recent decades for a wide variety of biomedical and industrial processes and considerable progress in research in this field has been seen, evidenced by the significant number of papers published over several decades, commercial products developed and marketed and which continuing to be produced. This work extends the body of knowledge in the field and focuses on two industrially-important 'chemical' measurands: the determination of pH level and oxygen concentration (O_2) - both are critically important for a broad range of applications globally, in fields as diverse at the life sciences, environmental monitoring, biomedical research and thus widely across industry.

The many different optical platform designs and fabrication methods that have been developed are considered, including those for commercial applications, recognizing the wide range of industrial and scientific uses, and their performance compared. Further, the effect of specific fiber structures on sensor performance, e.g. on sensitivity, response time and long-term stability, and possible applications also has been analyzed. Applications are seen in difficult and 'niche' measurement environments to which conventional sensors are often not well suited, taking advantage of their lightweight nature, ease of miniaturization, potential to be multiplexed and low cost. Through a discussion of representative techniques that have reached commercial development, a comprehensive and state-of-the-art view of this exciting and important field is possible.

1   Introduction

The determination of the pH level and oxygen concentration (O_2) are very important across a broad range of applications today: in life sciences, environmental monitoring, biomedical research and widely in industry globally. For example, there is particular interest in detecting both parameters in areas as diverse as the clinical analysis of blood [1], for quality control in the food industry [2], for process control in bioreactors [3, 4] or seawater analysis [5, 6]. In bioreactors, for example, pH (typically ~7.6 ±0.1 pH for most animal cells), dissolved oxygen [7] and temperature (30°C - 40°C) are the three crucial parameters to control the cell growth and keep the cells staying alive. Further, the trend in bioreactors seems to have shifted recently from fixed to single-use reactors; a change that highlights the need for small sized, miniaturized and less expensive sensing concepts [8]. McLeod et al. have shown the need for oxygen sensors in a climate change study to analyze effect of ocean warming and changes to food supply of larval coral reef fishes [9]. Other measurements in aquatic systems require fast and small oxygen sensors (samples rates from 16 - 64 Hz.) to monitor oxygen fluctuations across the sediment-water interface which is relevant for the eddy covariance correlation technique [10, 11].

Classical electrochemical sensors, such as the Clark electrode [12] and the pH glass electrode [13], are well known for the measurements of O_2 concentration and the value of pH. However, these types of sensors have the disadvantages of being potentially subject to interference from stray electromagnetic fields and as they consume the sample (analyte); these features can cause problems in some important industrial monitoring situations. In addition, they often are bulky and their glass surface makes them fragile and subject to breakage, unless they are handled carefully – not the case in many industrial situations. Optical, and especially fiber optic sensors have become attractive for these sorts of measurements in recent times since these sensors *do not* consume the analyte (e.g. oxygen), they are reversible and easy to miniaturize (< 50μm) due to the use of small diameter fiber. Further, they can be used to measure the analyte in *either* the gas or the liquid phase, they are inexpensive (due to the low cost of fiber and the small sample of sensitive material used) and can be employed where electromagnetic interference would mean that conventional sensors would fail. Therefore, there is increasing demand for such fiber optic pH and O_2 sensors, addressing an ever-expanding range commercial and industrial uses. Since the year 2000 the *commercial* success of such sensor systems is evidenced by a growing number of companies that manufacture sensors and sell instrumentation systems in these areas: examples from different countries globally include PreSens Precision Sensing GmbH (www.presens.de), Ocean Insight Inc. (www.oceaninsight.com), World Precision Instruments Inc. (www.wpiinc.com), PyroScience GmbH (www.pyroscience.com), Unisense (www.unisense.com), Ohio Lumex (www.ohiolumex.com) and many others, with new companies being formed on a regular basis, often as University 'spin outs' or 'start-ups'.   As a result, a large number of commercial products offering different designs are available; designs that can successfully be applied to a broad range of applications. Examples of these include fiber optic sensors with small sensor tips < 50μm, ideally suited to measurements of very small volumes e.g. for biomedical fluids or 'lab-on-a-chip' (Figure 1A), sensor 'spots' for the direct monitoring of samples in glass vials (Figure 1B), or robust designs for wider potential industrial uses (Figure 1C). Given the importance of the variety of commercialized sensors for industrial applications, a more detailed overview of the wide range of available systems and sensors can be found in Section 6, in this way to help the experimenter seeking to find the optimum device for any specific application.
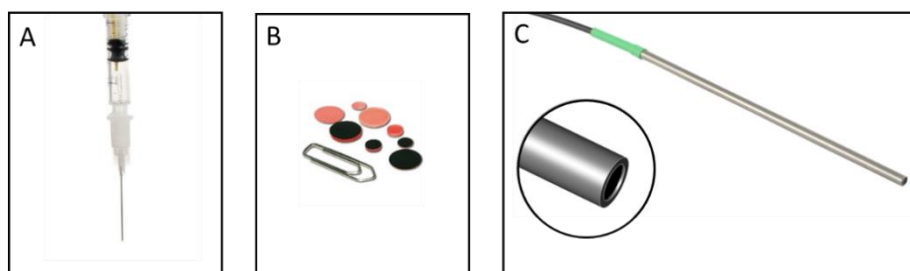
Figure 1: Examples of commercially available optical sensor designs. **A**: fiber optic O₂ sensor (tip < 50µm) in a syringe housing (www.wpiinc.com); **B**: O₂ sensor spots for glass vials (www.presens.de); **C**: pH sensor with a stainless steel housing and a diameter of 3 mm (www.pyroscience.com).

Figure 2 shows a schematic of the basic components of an optical (or fiber optic) sensor system, including the analyte, the optical platform, and signal processing (electronics and software) to convert the optical signal and display the analyte concentration. In general, an optical sensor system needs an indicator dye that changes its optical properties in a readily detectable way, when interacting with the analyte of interest. Typically the indicator dye used in such applications is held or immobilized in a supporting matrix (e.g. polymers, sol-gels and hydrogels) that needs to be permeable to the analyte [14–18]. There are three widely used methods for the immobilization of a dye in a solid matrix: adsorption, physically entrapment and covalent binding. Compared to the other techniques, covalent binding is usually complex and time-consuming and needs an appropriate material suitable for the immobilization. However, for some sensing concepts and where dyes are used as pH-sensitive materials, covalent binding is often preferred to eliminate leaching effects [19]. The sensitivity to an analyte usually depends on both the dye and the matrix characteristics, e.g. its density, viscosity and hydrophobicity. Therefore, the intrinsic properties of both, dye and matrix, must be considered together when fluorescence-based oxygen or pH sensors are to be developed. Once an appropriate material has been identified, the aim is for the sensing element to be applied to the most appropriate of several potential optical platforms (e.g. optical fibers, glass plates and capillaries) using a suitable coating procedure amongst which the most popular are dip coating, spin coating or photo-polymerization. Depending on the dye and sensing methodology, the measured signal change could be as a result of different interactions, such as absorbance/reflectance, luminescence (intensity or lifetime) or for some multiple sensing concepts, a combination of both. In addition, monitoring of refractive index, light scattering, and light polarization have also been used as analytical parameters which can be related to other measurands. As an example, the most widely used technique to detect oxygen is to measure the change of luminescence *lifetime* that is influenced by the quenching rate of the excitation state. To describe the photophysical effect caused by collision quenching by O₂, the most familiar approach is through using the Stern-Volmer equation. A detailed description of this approach can be found in Section 3, including a discussion of additional quenching models and sensors available using this approach.

While several earlier reviews have previously covered this specific field e.g. [15, 16, 18–22], there has been considerable progress since many of these were published which needs to be considered. Thus it is a good time for reporting of the field to be updated, illustrating the need for a new review to focus on recent advances that have influenced it, especially as a result to include developments in sensing methodologies/instrumentations (Section 4) and the wider variety of optical platforms currently available, as well as developments in sensitive materials and immobilization methods, many of them commercially. To do so, this review analyzes the breadth of work which has been published recently, as a result to review activity across a variety of optical sensing platforms, with the focus on fiber optic luminescence based O₂ and pH sensors, a very important topic for industry (Section 5 & 6). The key aim, in this way, is to make the scope to what can reasonably be covered more readily comprehensible and comparable, yet ensure the value of the work which is both comprehensive and topical. Thus not only will it investigate the research work in this field recently published but in particular it will extend this to look at and cross-compare commercial

developments that have built on these (Section 6). The final section highlights further trends in optical O_2 and pH sensing and provides some future perspectives for the field. To provide a basis for the work that follows, a brief theoretical background to optical O_2 and pH sensing is given in Section 3.

Sample of Interest
› oxygen dissolved and/or in gas phase
› pH in liquids
› or others (e.g. ammonia and CO_2)

Coating Platform
› coating applied on optical platform (e.g. optical fiber, glass plate or capillary)
› interface between coating material and instrumentation

| Analyte | Sensitive Coating | Optical Platform | Signal Processing | Analyte Concentration |

Sensing Element
› indicator dye immobilized in an analyte permeable supporting matrix (e.g. polymer, sol-gel or hydrogel)

Instrumentation
› conversion of optical signals
› optical components, electronics and software
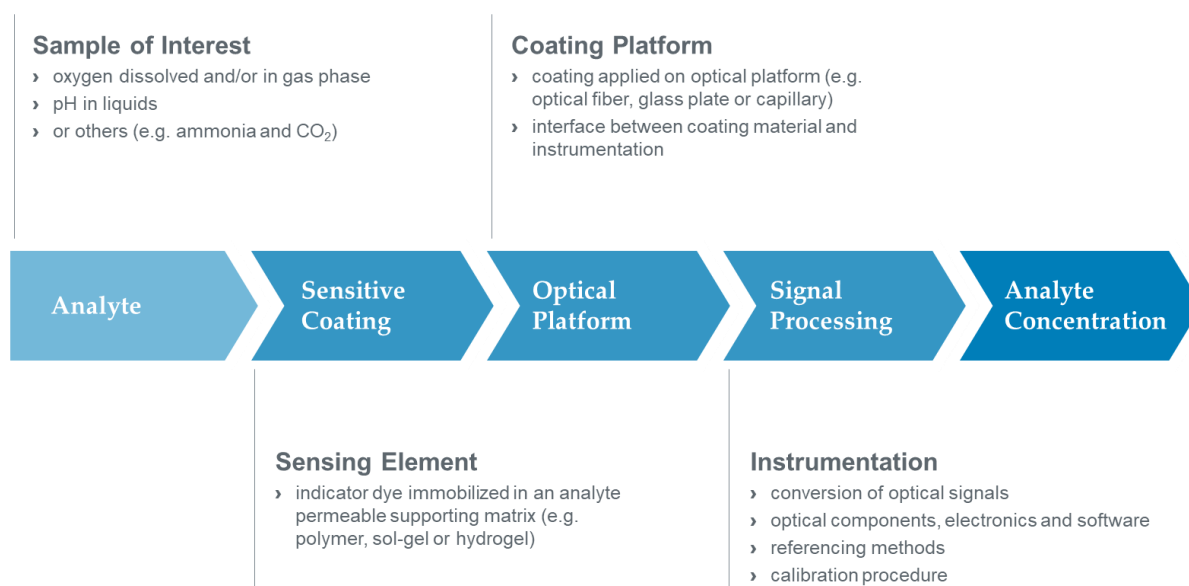› referencing methods
› calibration procedure

Figure 2: Schematic of an optical sensor system showing all necessary components.

2   A Looking Back – The Timelines for Key Developments in the Field

Quenching of luminescence by oxygen or other quenching species has been known for a long time, but was first described by Stern and Volmer through their famous equation. Fifty four years after that, in 1973, Lakowicz and Weber developed a high pressure fluorescence cell and associated instrumentation to measure the effect of the quenching of fluorescence intensity by oxygen [23]. That work was a milestone in the field and proved to be the basis for all subsequent optical sensors using this physical effect. Thus in 1974, Hesse patented a fiber optic oxygen sensor to measure the fluorescence intensity or fluorescence decay time of an oxygen-sensitive chemistry placed at the end of a single optical fiber or fiber bundle [24]. At the time, this represented a very new approach and appears to be the first fiber optic chemical sensor to be reported.

In 1984, Peterson et al. were able successfully to measure the oxygen concentration in blood using one of the first fiber optic chemical sensor designs in a biomedical application [25]. In this design, one polymer fiber was used to guide the excitation light to the oxygen-sensitive porous polymer tubing used, with a second being necessary to guide the emission light generated to the detector. This critically showed the possibilities of such a design of optical sensor, with applicability to biomedical research especially for *in vivo* measurements of oxygen partial pressure. To overcome the issue of poor long term stability, which is a feature due to photobleaching seen in such published optical oxygen sensing concepts, Lippitsch et al. have described an enhanced design of optical sensor for oxygen which has a detection system that is based on the measurement of the fluorescence *lifetime* rather than *intensity* [26]. Such a scheme used a novel ruthenium-based indicator, firstly described by Wolfbeis et al. [27]. The novel indicator showed a better quantum yield and usefully a relative long decay time (in the microsecond region) which was ideal for making an accurate measurement more easily, suiting this sensing purpose very well. Since that time, significant research efforts have been made to develop both new oxygen-sensitive indicators and supporting materials to optimize sensor performance, e.g. enhance photostability and/or decay times. In 1997 Sang-Kyung Lee et al. developed an oxygen-sensing material based on platinum tetrakis(pentafluorophenyl) porphyrin (PtTFPP) which was immobilized in a polystyrene (PS) polymer [28]. This indicator has demonstrated

an improved photostability and resulting reliability in use, compared to the better known PtOEP [29, 30]. Further, PtTFPP showed a strong emission intensity and long decay time, in the microsecond region, which was very advantageous in the sensor design. During ~50h continuous irradiation of the PtTFPP-based material, the emission intensity decrease was only 9.2% compared to a decrease of 46.5% when using PtOEP in a similar experimental set-up. Klimant et al., however, have developed the first reliable fiber optic O_2 microsensor [31] and introduced a suitable detection system for it [32]. Due to the greater ease of manufacturability, compared to traditional small sized Clark electrodes (< 5μm), an enhanced 'shelf-life' stability (> 6 months) and the less expensive components used in the whole system it was a milestone for the commercialization of these new fiber optic O_2 sensors.
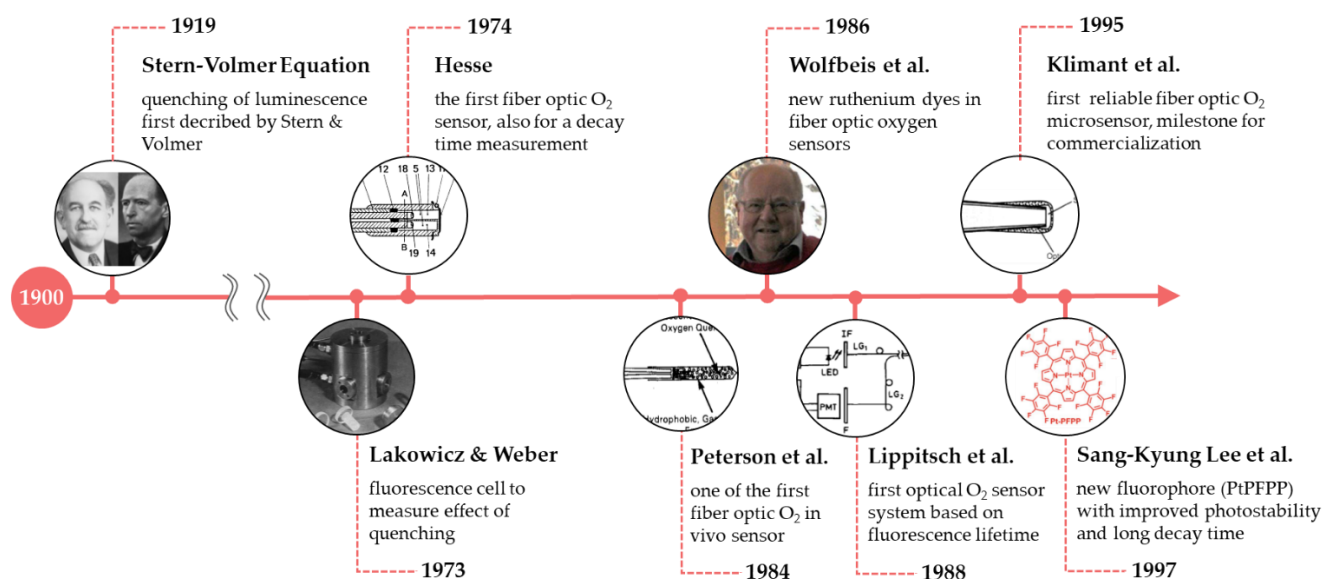

Figure 3: Timeline of milestones in the development of optical O_2 sensors [15, 23–25, 29, 31, 33–35].

When the first optical pH sensors were developed is not clear - however, universal indicator dyes were firstly patented by Yamada in 1933 and described in experiments by Laurence S. Foster and Irving J. Gruntfest in 1937 [36]. Therefore, using a color change to measure pH became a very well-known approach to pH monitoring using familiar 'test strips' and this is still the most widely used method. Here an indicator dye is linked to a reagent paper and it is likely that the first pH indicator paper was patented by Henry Wenker in 1938 [37]. As a consequence, the idea of the immobilization of an indicator could then be extrapolated to create a fiber optic sensor used for the continuous monitoring of pH. Peterson et al. described the first fiber optic pH sensor system based on two polymer fibers with sensing particles in a cellulosic tubing attached at the end in 1980 [38]. This initial development increased the interest in this instrumentation and was a start for a significant number of new developments, creating several publications in this new field. In 1982 Saari et al. described the first optic pH sensor system based on a fluorescence intensity measurement and showed the potential of *binding* an indicator dye (fluoresceinamine) in a supporting material (cellulose) that is attached to the end of a fiber optic [39] (Peterson's work linked the indicator to sensing particles and not to the fiber itself). In that same year Tait et al. demonstrated the possibility of using a small fiber optic pH sensor in an *in vivo* measurement - clearly what is critical here is avoiding any damage to the living organism due either to the indicator crossing from the sensor to it, or any breakage of the fiber creating a sharp edge. During the measurements in a beating heart, a comparison was made of the new sensor developed and a reference glass electrode which were used and showed similar responses to the pH of the environment. Looking for new pH sensitive indicators that were suitable for use in the physiological range from pH 6.5 to 8.5 encouraged Zhujun et al. to describe a new dye, HOPSA (HPTS), loaded in a membrane [40]. Further, they introduced a

ratiometric fluorescence measurement to reduce the effect of instrumentation fluctuations (such as is caused by changes in the light source or bending of the fiber) and this increases the precision of the sensor and reduces errors. To reduce the complexity and costs of previously described instrumentation designs Grattan et al. published a new approach to measure the reflectance change of a pH indicator with an improved system [41]. To do so, the authors developed and compared two different referencing methods (a two-LED reference system and a fluorescence reference system) to reduce the effect of any fluctuations of the light sources on the measurement made with the whole system. In 1988 Knobbe et al. fabricated a porous silica as supporting material for an indicator dye and demonstrated that organic dyes are compatible with the sol-gel synthesis technique [42]. Further, no dye leaching was observed, critically important for many applications which could not be 'contaminated' by the indicator dyes (many of which were carcinogenic), especially in light of *in vivo* applications. Compared to polymers, sol-gels have several advantages, which include better transport properties and stability in harsh environments, which makes them very good host materials (and not only for pH-sensitive dyes but for other indicators as well e.g. oxygen monitoring). However, problems with cracking and long term storage of sol-gels were seen in some early work [43–45]. One of the first durable ratiometric pH microsensors (with a very small tip size, < 2µm) for physiological measurements (pH 6.3 - 8.4) was developed by Song et al. in 1997 [46]. This fiber optic pH sensor was based on a new single-excitation/dual-emission design that showed a fast response time, high precision and, importantly, was reversible. Further, the authors demonstrated that a repeatable manufacturing of this fiber optic pH sensor design was possible - this making it a milestone for following the commercialization of such products, where many sensor probes, with the same and reproducible characteristics, are needed. In 2001, and years after the first time-domain fluorescence-based pH sensor was published [47], Klimant et al. reported a new detection scheme based on a dual lifetime referencing (DLR) method [48]. This was introduced to overcome the effect of photo-bleaching of the indicator dye during measurements, a problem that was seen to occur when high power, short wavelength sources were used in the sensing design. Ultimately, this measurement technique was applied in one of the first commercially available pH systems from PreSens (www.presens.de).
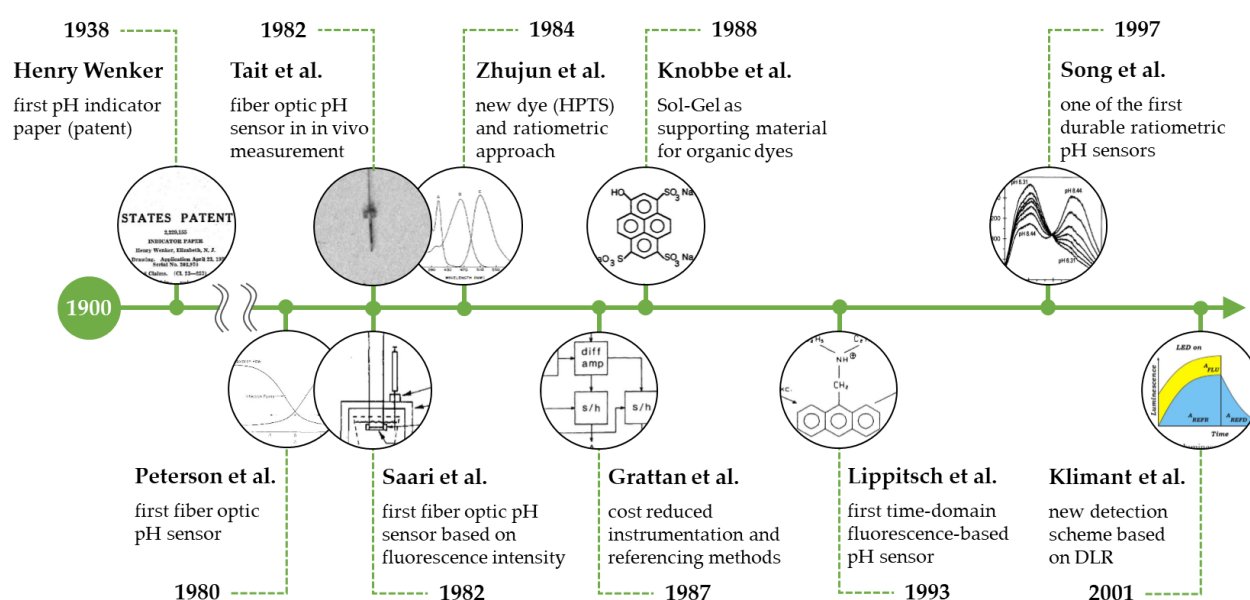

Figure 4: Timeline of milestones in the development of optical pH sensors [37–42, 46–49].

3 Theory and Background of Optical O_2 and pH Sensing

This section shows an overview of the essential fundamental theory of photoluminescence and the important physical processes involved when using luminescence-based indicators as sensing elements in instruments within the scope of this work, noting that a more detailed description can be found in the references attached.

3.1 Photoluminescence

Photoluminescence is a well-known process involving the emission of photons and occurs when a luminescent molecule is excited with light of a wavelength which is suitably absorbed and, through internal processes, induces emission at specific and known wavelengths. Typically in organic materials, the molecule absorbs a photon and is excited from the ground state (labelled S_0) to higher vibrational energy levels (0, 1 or 2) of the electronic states S_1 or S_2. The various molecular processes appearing in the excited states concerned can usefully be illustrated through the so-called Jablonski Diagram (see Figure 5). This illustrates well a number of interactions, such as energy transitions (vertical lines) between the electronic states (horizontal lines) and quenching, to describe the nature of light absorption, emission and several important internal effects that affect the performance of the molecule, and thus its value for use in a sensor system. After absorption takes place, the molecule first relaxes to the lowest vibrational level S_1 and then internal conversion takes place. From electronic state S_1 two major radiative processes are possible before returning to ground state, resulting in the emission of either fluorescence or the longer-lived phosphorescence emission. Fluorescence has a high probability of occurrence but molecules of state S_1 also can undergo a conversion to the first triplet state T_1 (due to intersystem crossing). In the more efficient fluorescence-based sensor systems, the phosphorescence should be minimized as it has a lower energy and therefore shifted to a higher wavelength relative to the fluorescence spectrum – it represents a 'loss mechanism' that is undesirable in an efficient sensor system [50].

Comparing the absorbance with the emission spectrum (fluorescence and/or phosphorescence) the luminescence typically has a lower photon energy and is shifted to a higher wavelength. This phenomena is termed the Stokes-Shift, illustrated below for Rhodamine B in Figure 6, and was firstly observed and published by Sir George Gabriel Stokes in 1852 [51]. However, the nature of this Stokes-Shift is only one important parameter when selecting a luminescence-based dye as the sensing element – it does mean that optical filters can be used to eliminate the effect of what is often powerful light from the optical source (by comparison the fluorescence emission) on the optical detector used. Thus a larger shift of the luminescence spectrum relative to the absorbance wavelength is frequently seen, since this allows a better separation of excitation and emission light using optical filters, allowing for greater efficiency and therefore reduced costs of the optical setup, this positively influencing significantly the design and optimization of the whole instrument developed.
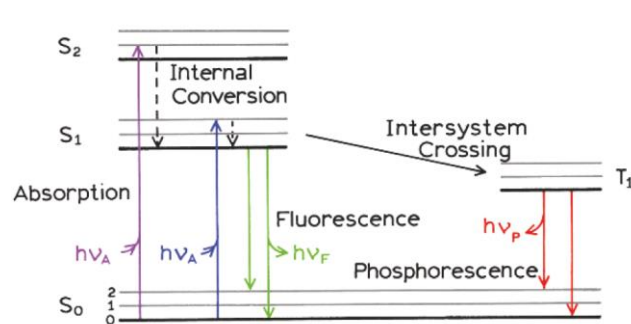

Figure 5: Jablonski Diagram illustrating the effect of absorption and photoluminescence. S_0, S_1 and S_2 are the electronic states and T_1 is the first triplet state [50].
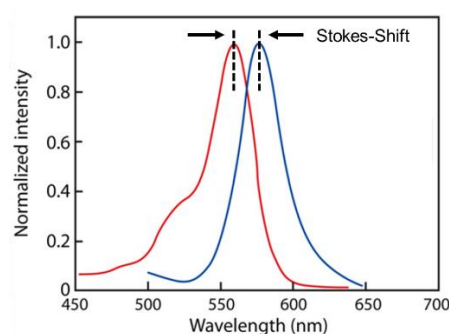
Figure 6: Stokes-Shift exemplary showing the normalized absorbance (red) and emission (blue) spectrum of Rhodamine B in PMMA (based on [52]).

3.2 O₂ Quenching and widely used Models

The photoluminescence seen from many materials can be influenced by various processes and these can form the basis of an effective sensor system - such changes are termed quenching. Thus in the presence of molecular O₂, the luminescence intensity and life time is reduced due to dynamic collisions of the O₂ molecules in the excited electronic state S_1 (see Figure 7); the fluorophore returns back to ground state S_0 without the emission of a photon. This process is fully reversible and does not chemically alter the molecules involved [15, 50].
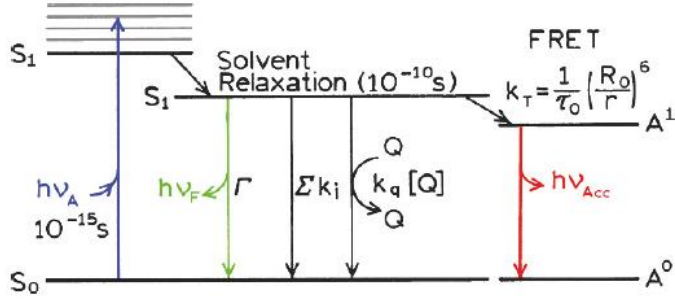

Figure 7: Modified Jablonski Diagram describing the effect of collision quenching and FRET [28].

To describe the photophysical effect caused by collision quenching by O₂, the most familiar approach is through the so-called Stern-Volmer equation mentioned above:

$$\text{Stern-Volmer:} \qquad \frac{I_0}{I} = \frac{\tau_0}{\tau} = 1 + K_{SV}[O_2] \qquad (1)$$

where I_0 is the luminescence intensity and τ_0 the life time in the absence of O₂, I is the luminescence intensity and τ the life time in the presence of O₂, K_{SV} is the Stern Volmer constant, while $[O_2]$ is the concentration of the quenching agent (O₂).

However, the Stern-Volmer equation is only fully valid for an ideal quenching system. Since many luminescence materials used as sensor coatings show non-linear behaviors, two other models (Lehrer and Demas) are well-known and can be used to describe the effect of a quenchable and a non-quenchable site:

$$\text{Lehrer:} \qquad \frac{I_0}{I} = \frac{\tau_0}{\tau} = \left(\frac{f}{1 + K_{SV}[O_2]} + (1 - x) \right)^{-1} \qquad (2)$$

$$\text{Demas:} \qquad \frac{I_0}{I} = \frac{\tau_0}{\tau} = \left(\frac{f}{1 + K_{SV}^1[O_2]} + \frac{(1 - f)}{1 + K_{SV}^2[O_2]} \right)^{-1} \qquad (3)$$

where K_{SV}^1 and K_{SV}^2 are the Stern–Volmer constants for the two sites, f and (1 − f) represent the relative contribution of each site to the total emission of luminescence. In the Lehrer model, the constant of the second site (K_{SV}^2) is assumed to be null. Medina-Rodríguez et al. has published a detailed study comparing all three models, involving data from actual experiments and using different criteria for the calibration of photoluminescence-based sensors, all designed to minimize the error in the measurement made. Further, they provide suggestions on the optimization of the implementation of the calibration procedures, as well as on the development of a suitable software code [53].

3.3 Förster Resonance Energy Transfer (FRET)

In comparison to a single luminescence measurement (intensity or lifetime) FRET offers a ratiometric approach for an optical sensor design and is another electrodynamic process that can occure in the excited state (see Figure 7). This physical phenomenon, also known as RET (resonance energy transfer) or EET (electronic energy transfer), is named after Theodor Förster who described an improved theoretical treatment in 1948 [54]. It is a non-radiative process and occurs whenever an excited molecule, so-called donor, transfers its energy to an acceptor molecule through dipole–dipole interactions. Here, the emission spectrum(s) of the donor must overlap with the absorption spectrum of the acceptor (see Figure 8) [50, 55].
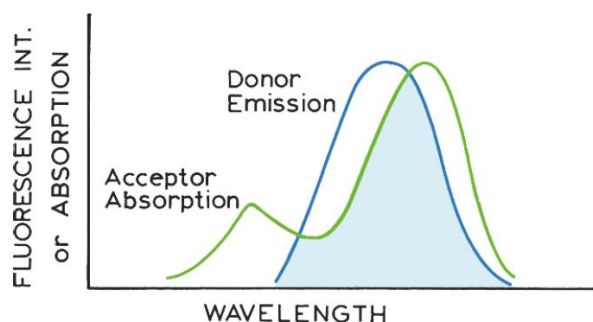

Figure 8: Spectral overlap of the emission (donor) and the absorption signal (acceptor) [50].

Described in the famous equation of Theodor Förster (equation 4) , the rate of energy transfer $k_T(r)$ is determined by the distance r between the donor (D) and the accpetor (A), and the extent of spectral overlap. The overlap bewteen the fluorescence spectrum of donor and absorption spectrum of the acceptor is given by the well-known Föster distance R_0. Here, τ_D is the lifetime of the donor in the absence of energy transfer [50].

$$k_T(\mathrm{r}) = \frac{1}{\tau_D}\left(\frac{R_0}{r}\right)^6 \tag{4}$$

Since FRET is large and complex, e.g. different for donors and acceptors covalently linked or free in solution, extended versions of equation 4 are necessary to descirbe these effects. Further, details of the fundamental theory can be found in the literature, [55].

3.4 Definition of pH and the Henderson-Hasselbalch Equation

The pH scale was introduced by Søren P. L. Sørensen in 1909 where firstly pH was described as the negative logarithm of hydrogen ions concentration [56]. Nowadays pH is defined in terms of hydrogen ion activity a_{H^+}:

$$\mathrm{pH} = -\log a_{H^+} \tag{5}$$

Classical electrochemical sensors directly measure the activity of hydrogen ions in aqueous solutions and optical pH sensors the concentrations of the protonated and deprotonated form of the indicator dye. For luminescence-based sensors, this effect results in a change of the luminescence intensity observed. The well-known Henderson-Hasselbalch equation is commonly used to determine pH from the changes of the deprotonated [A-] and protonated [HA] form optically [19] where:

$$\mathrm{pH} = \mathrm{pK_a} - \log\frac{[\mathrm{HA}]}{[\mathrm{A}^-]} \tag{6}$$

and pK$_a$ is the acid-base constant of the indicator dye.

Defining I$_{max}$ as the maximum luminescence intensity signal of the deprotonated form and I$_{min}$ as the minimum luminescence intensity signal of the protonated form, the value of pH can be calculated using the following equation:

$$pH = pK_a - b \cdot \log\left(\frac{I_{max} - I_m}{I_m - I_{min}}\right) \tag{7}$$

where I$_m$ is the measured luminescence intensity and b the numerical coefficient to determine the slope of the function [57].

4   Sensing Methodologies and Instrumentation for O$_2$ and pH monitoring systems

Many luminescence-based measurement techniques have been developed in the past and, depending on the requirements of the whole system and the application, they are available showing different levels of complexity. This section gives an overview of the state of the art 'readout' schemes from the basic and less expensive instrumentation to the complex set-ups for multiple sensing methodologies. In general, an instrument for luminescence-based sensors consist of three main parts: (i) an indicator or sensing layer; (ii) an optoelectronic system to measure the luminescence; and (iii) a suitable software for signal processing. This optical concept has not really changed since the very beginning of optical luminescence-based sensors and it is still an important basis for future developments in the field. However, further improvements to the designs have been published since that time, with a view to optimize the whole system performance (e.g. involving long-term stability, accuracy and response time) and including the sensor, the optical and electronic set-up and the software designed and used. Further, new referencing methods have been described in many of the following papers, with the goal to reduce system fluctuations and/or minimize cross-sensitivities of the sensors to other parameters such as temperature, pressure or non-desirable chemical reactions to other substances. The following subsections will address these sensing principles with the focus on O$_2$ and pH, and discuss the different instrumentation designs of devices that can be used to make such measurements most effectively in industry today and into the future.

4.1 Single Luminescence Intensity sensing Concepts

The measurement of a luminescence intensity change is the simplest way to detect the concentration changes of an analyte (here focused on pH and O$_2$ detection) when using luminescence-based optical sensors [31, 39, 58, 59]. The intensity changes related to oxygen are very well known and described in the Stern-Volmer equation and the changes to pH can be described using the Henderson-Hasselbalch equation (see Section 3). The advantages of a single intensity measurement are that it doesn't require a complex instrumentation including the optical set-up, electronics and software, and only one indicator dye is required. The recording of the intensity can be performed in the spectral domain (when using a spectrometer) or at a specific wavelength (when only a photodetector is required). A typical set-up to detect the spectral change is shown in Figure 9. Here the authors used a LED to excite the fiber-optic pH sensor at a wavelength of $\lambda_{exc.}$ = 380 nm, where the novel, recently developed coumarin dye has its absorbance maximum [60]. In comparison to lasers and other light sources (e.g. halogen or xenon lamps) LEDs are favorable since they are low in price, small in size, have less power consumption and can be easily modulated [31]. A fiber coupler is used to guide the excitation light to the tip of the fiber-optic sensor with the pH sensitive layer attached and a portion of the luminescence emission (at $\lambda_{em.}$ = 535 nm) is collected and guided through the other branch of the fiber coupler to a spectrometer. A fiber coupler is a very common way to split the beam and route light to different channels and is used in many other published luminescence

detection systems [10, 31, 39, 61–63] as well as in different types of commercial instrumentation (see Section 6.2). Using a beam splitter (dichroic mirror) is another very efficient possible way to separate light and has the advantage of allowing a direct filtering of the excitation and emission light [64]. However, compared to a fiber coupler dichroic mirrors are typically very expensive and other optical components like lenses are required in the optical set-up. That increases the costs significantly and is less suitable and convenient, especially when the overall price needs to be kept low. The spectral changes to pH and titration plot measured are shown in Figure 10. Since this coumarin dye shows a relative strong emission intensity and a relative large Stokes-Shift of ~155 nm an optical filter is not absolutely required in this set-up to separate the emission from the backscattered excitation light.
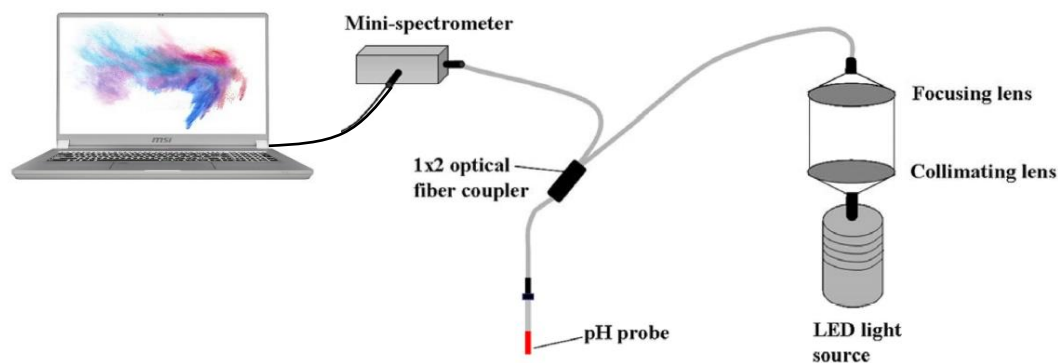

Figure 9: Example of an optical system for a fiber-optic pH sensor based on a spectral luminescence intensity measurement using a spectrometer [60].
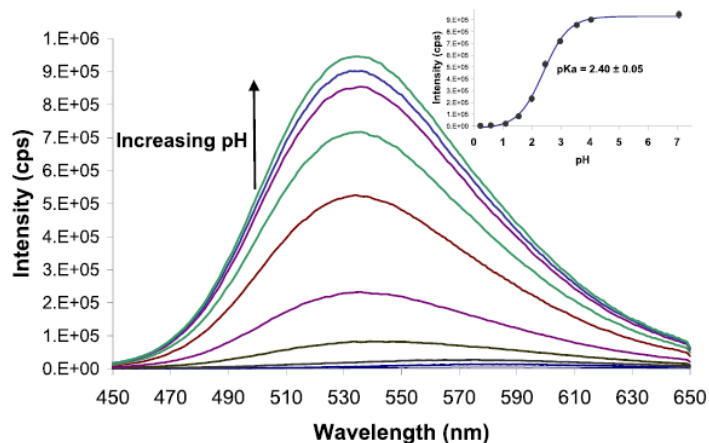

Figure 10: Measured spectral response to pH and titration plot of fiber-optic pH sensing system shown in Figure 9 [60].

For continuous monitoring applications, a detection system with a photodetector is recommended to measure the luminescence intensity changes at a specific wavelength. In the literature [65], the authors describe an optical set-up for a pH flow cell sensor with the pH sensitive coating on a PVC substrate (see Figure 11). This shows a typical set-up and this can be transferred to other optical platforms (e.g. fiber optic sensor designs) or other indicator dyes [66–68]. A blue LED ($\lambda_{peak} \approx 480$ nm) is used to excited the indicator dye (fluorescein O-methacrylate) that is covalently linked to a hydrogel matrix. Since the intensity of the excitation light is typically relatively high compared to the emission light of a luminescence indicator a short pass filter ($\lambda_{cutoff} = 485$ nm) is placed between the blue LED and the pH sensitive layer. Further, a bandpass filter ($\Delta\lambda = 515 - 535$ nm) between the pH sensitive layer and the photodetector is necessary to block most of the backscattered

excitation light. In addition, using a bandpass filter instead of a long pass filter has the advantage of reducing the effect of stray light that might be an issue for some sensor designs when using it in a very bright environment and when an additional over coating (optical isolation) [69] is undesirable. In addition, if the used indicator has a relative large Stokes-Shift and strong emission light it is possible to use glass filters instead of expensive interference filters [31]. Since the emission light is typically very weak highly sensitive detectors like avalanche photodiodes, PMTs or SiPMTs are a suitable choice to use. The system drift in a single intensity measurement can be reduced or compensated by adding an additional photodetector (e.g. photodiode) closed to the light source. Measuring the excitation light and using it as reference for further signal processing is well-known and was used successfully in work reported in other publications. Further, using the lock-in technique (see Figure 12) increases the signal-to-noise ratio, especially when weak luminescence signals needs be measured. To reduce the effect of photobleaching of the indicator dye during a continuous measurement, it is possible to add on/off phases of the light source to the system (LED off when no sample point is taken). This will increase the lifetime of the sensor and reduce the signal drift related to the photobleaching.
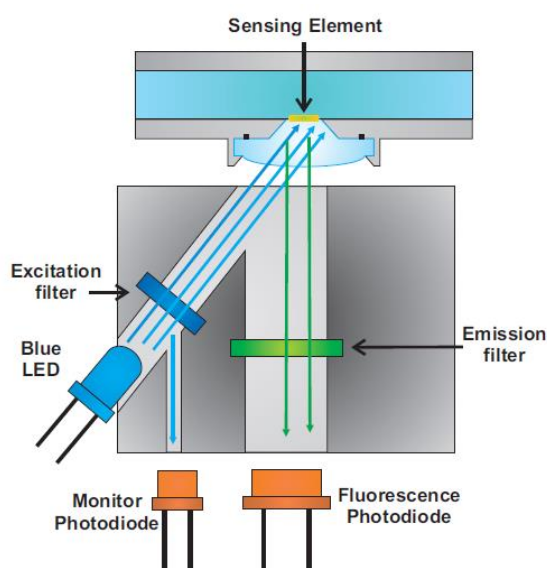

Figure 11: Example of an optical system for an optical flow cell pH sensor based on a luminescence intensity measurement using a photodetector to detect the luminescence emission and a reference photodiode for compensation [65].
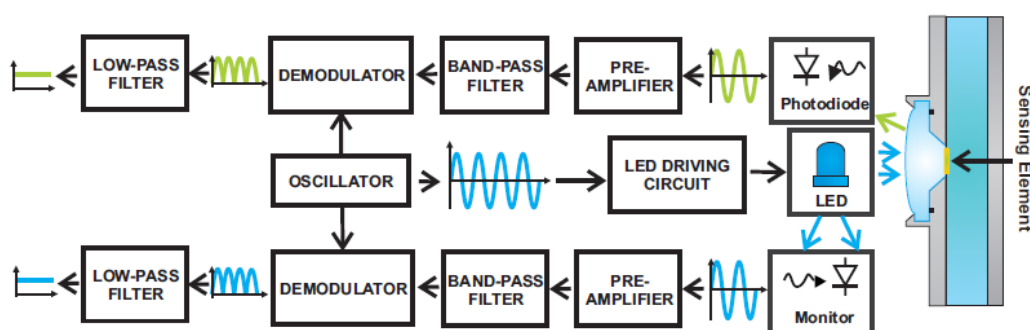

Figure 12: Schematic illustration of an electronic set-up using the lock-in technique and a compensation method for luminescence-based measurements [64].

4.2 Single Luminescence Lifetime and Decay Time Sensing Concepts

To overcome the issues/limitations of a single intensity-based measurement using only one indicator dye the most popular detection method is the measurement of the luminescence lifetime or decay time [15, 47, 68, 70, 71]. This parameter is independent to photobleaching, indicator concentration in the coating layer, drift of the light source and sensitivity of the photodetector. In particular, when using fiber optic sensors, the influence of fiber bending to the measured signal is typically small. The luminescence lifetime can be measured in the time-domain or the frequency-domain. In the frequency-domain method the excitation light typically is sinusoidal modulated and the emission of the indicator follows the modulation, but with a certain delay (see Figure 13, left). Then the lifetime τ is determined by measuring the phase shift between the excitation and the emission light. The relationship between the lifetime τ and the phase shift ϕ can be determined using the following equation [69]:

$$\tau = \frac{\tan \phi}{2 \pi f} \tag{8}$$

where f is the modulation frequency. However, in some cases the optimal modulation frequency can differ from the theoretically calculated [70, 72] but using equation 8 is a fast way for an approximately determination of the ideal frequency range.
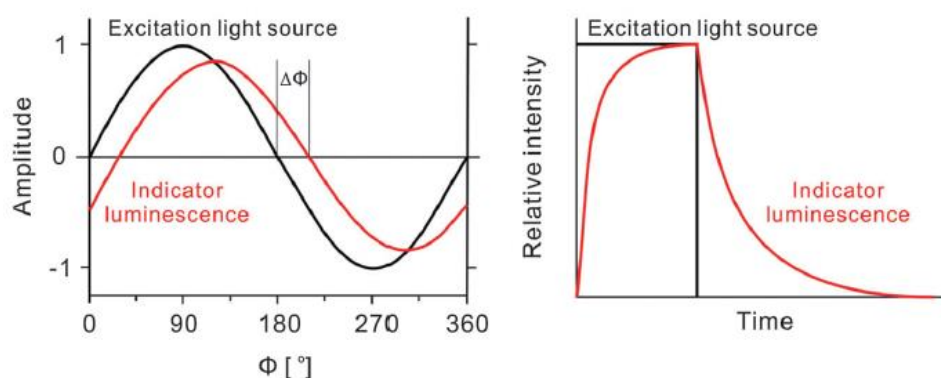

Figure 13: Principle of the frequency-domain method (left) where the indicator is excited with a sinusoidal modulated light (black) and the phase of the emission light is shifted related to the analyte concentration (red). Principle of the time-domain method (right) where the indicator is excited with a short light pulse (black). The emission light (red) increases to a steady-state and decreases delayed after the excitation source is turned off [15].

To keep the modulation frequencies relative low (in the kHz region), and thus reduce the complexity of the instrumentation, it is recommended to use long-lived metal-organic indicators with luminescence lifetimes in the µs region [73]. Examples of such O_2 indicators are PtTFPP, PtOEP, PdOEP and $Ru(dpp)_3^{2+}$. An overview of widely used O_2 indicators can be found in prior work [15–17]. In addition to a sinusoidal signal the light source can also be modulated with a square-wave function and using multiple modulation frequencies can increase the accuracy of the sensor system [74, 75]. The Medina-Rodríguez et al. have introduced a low-cost system for real-time measurements using an optical O_2 flow cell sensor and compared the multi-frequency I/Q method with the single frequency measurement during an experiment [76]. Schmälzlin et al. have developed a multi-frequency method to measure the intracellular oxygen concentrations in green plants [77]. The multi-frequency phase-modulation technique was used to discriminate the sensor signal from the strong auto-fluorescence of the plant tissue. They injected microbeads, including an O_2 sensitive

indicator (PtPFPP), into a Chara cell and measured the oxygen concentration directly with a microscope detection set-up.

In the time-domain method, the indicator is excited with a short light pulse (see Figure 13, right). The decay curve of the emission light could be measured using the time-correlated single-photon counting technique (TCSPC) that is based on the detection of single photons hitting the detector. In an ideal system the mono-exponential decay times can be fitted with a single-exponential function and the lifetime, τ, determined when the luminescence intensity drops $1/e$ of the initial value. However, this technique requires a fast and expensive instrumentation, needs exact synchronization of all components and the data processing is complex compared to the frequency-domain method [78]. An alternative time-gated methods is the rapid lifetime determination (RLD) where the decay time, τ, is integrated and determined by measuring the intensity drop in two successive time gates, labeled A_1 and A_1 (see Figure 14), and then calculated using equation 9. This method does not require an extreme fast and complex instrumentation, so is ideal for real-time measurements and shows a good level of precision and system accuracy [79].

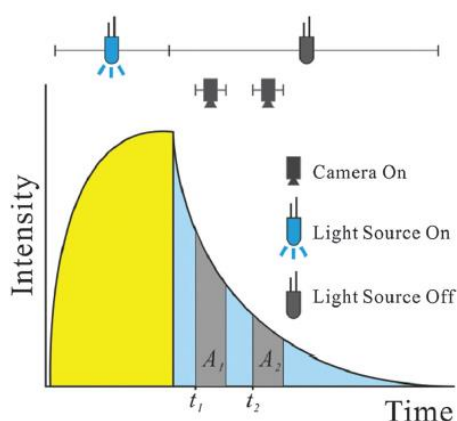$$\tau = \frac{t_2 - t_1}{ln\dfrac{A_1}{A_2}}$$

(9)

Figure 14: Principle of the rapid lifetime determination (RLD) method for a fast decay time determination over two time gates A_1 and A_2 [15].

Figure 15 shows a typical set-up for luminescence lifetime-based sensors using the frequency-domain method [61] but is also suitable for the time-domain measurement [48]. The set-up shown here is optimized for a fiber-optic sensor but can be transferred to other optical sensor designs (e.g. planar and flow cell sensors). The tip of the fiber-optic sensor was coated with an O_2 sensitive layer (ruthenium(II)-tris-4,7-diphenyl-1,10-phenantroline perchlorate immobilized in polystyrene) and connected via ST-adapter with the internal optical set-up. A blue LED ($\lambda_{peak} = 450$ nm) was sinusoidal modulated (f = 45 kHz) and the light routed through a 2x2 multimode fiber coupler to the O_2 sensitive layer on the fiber tip. An inexpensive glass filter was used to block undesirable longer wavelengths generated by the LED. The emitted luminescence light was guided back and routed through the other branch of the fiber coupler to a detector (PMT). A longpass filter was used to block most of the backscattered excitation light and transmit the luminescence light only. The other outcome of the fiber coupler was used as reference and to compensate phase/intensity drift and fluctuations of the developed system (generated by the light sources and electronics). The authors introduced two referencing methods for the phase detection. When using a photodiode only, the excitation light of the blue LED could be detected and used as reference for the electronic signal processing. A complex

electronical set-up is not required and the detection can be realized by using less expensive analogue circuits (see figure 16). A second possibility is using an additional red LED as a reference source. However, the signal processing is different since both LEDs run in a time-division multiplexing mode (the excitation LED and the reference LED are switched on alternately). The advantage of this method is that the whole optoelectronic path is then referenced. In addition, a comparable set-up was successfully used by the authors for other indicators (O_2 and temperature sensors) [32, 80] and in a multiple sensing concept for O_2 to measure the distribution of oxygen in a gas chamber [81]. Further, they could transfer this instrument design to detect pH with a fiber-optic sensor using the Dual Lifetime Referencing (DLR) scheme (details in Section 4.3) [48]. Since this detection system is ideal for a portable device (because of the small sized and relatively inexpensive components used), flexible to adapt to other sensors, fully characterized and successfully used by the authors over many years, it was patented in 2001 [82] and later became a commercial product (see Section 6).
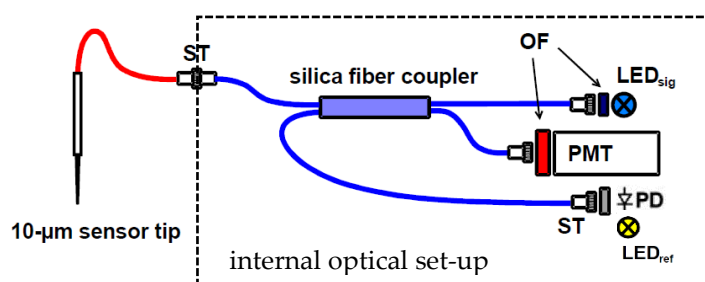

Figure 15: Optical set-up of a luminescence lifetime-based detection system with a fiber-optic O2 sensor connected and ideal for the realization of a portable device. Internal optical components: ST = optical ST-connector, OF = optical filters, PD = reference photodiode, LED$_{sig}$ = Excitation LED, LED$_{ref}$ = reference LED, PMT = photomultiplier [61].
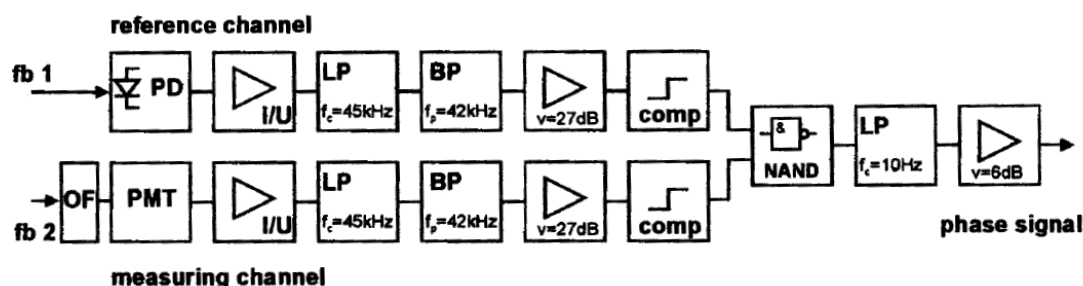

Figure 16: Schematic illustration of a low-cost electronic phase detection system (analogue signal processing) usable with the optical set-up in Figure 15 and showing the referencing method using a photodiode (PD). With: fb 1 = fiber 1 of a fiber coupler, fb 2 = fiber 2 of a fiber coupler, PMT = photomultiplier [61]

Wang et al. have proposed a low-cost and robust phase demodulator using commercially available ICs which are suitable to measure the phase shift of a fiber-optic luminescence sensor [83]. The electronical set-up is a based on a developed self-gain module (electronic circuit published in [84]) and was characterized and calibrated with a commercial lock-in amplifier. Further, the system was evaluated during an experiment using an optical fiber bundle and a commercial sensor patch that is sensitive to O_2 (RedEye, Ocean Optics). The demodulator shows a really good linearity, long-term stability and phase resolution of 0.02°. The experiments showed that the phase noise increases from ±0.03° (@ 0.99 %O2) to ±0.08° (@ 5 %O2) which means an oxygen fluctuation of ± < 0.005 %O2 and ±0.13 %O2 respectively. However, other developed systems show a better signal-to-noise ratio (see Section 6) but this inexpensive approach and less complexity offers a new opportunity for low-cost and small-sized sensor designs (e.g. wearable sensors). Chu et al. had followed the same idea of a

low-cost and small phase shift detection system but coated the photodetector directly with an O_2 sensitive film (PtPFPP in a polymer matrix) [71]. The set-up developed does not require optical filters, and low-cost ICs were used in the electronic circuit (see Figure 17). Further, the authors characterized the sensor system in a test chamber for O_2 concentrations from 0% to 100% and a temperature range from 25°C to 55°C. The sensor displayed a maximum phase shift difference of 18° between 0% and 20% O_2 with a resolution of better than ±2% O_2. This is not very accurate, however, it can be a very low-cost alternative for some applications (e.g. in the food industry or for environmental monitoring).
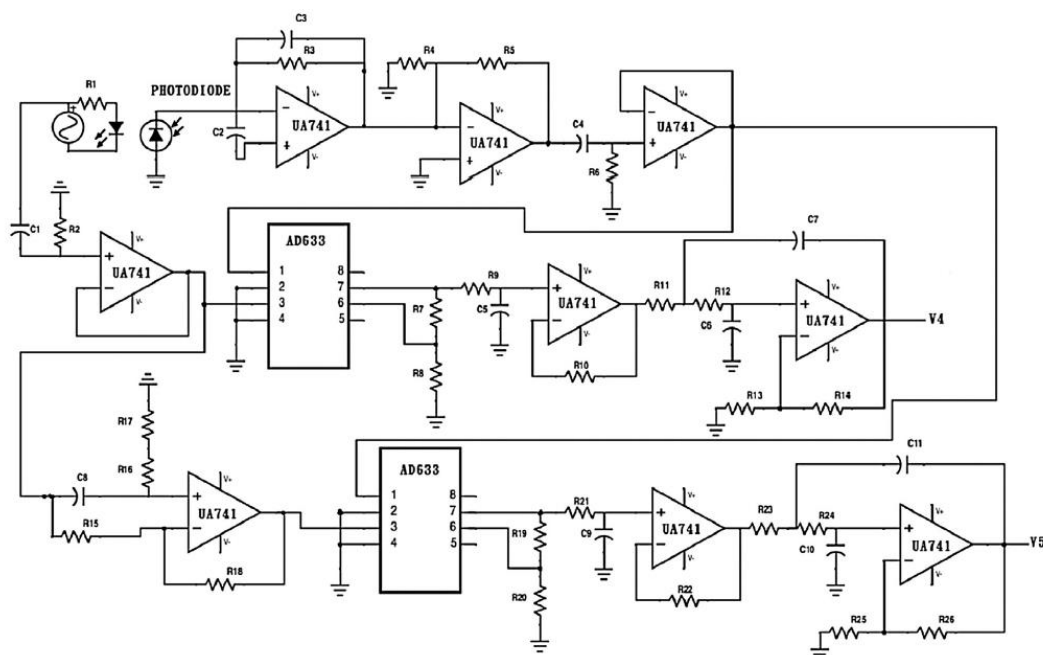

Figure 17: Electronic circuit of low-cost luminescence phase detection system for a photodetector (photodiode) directly coated with an O_2 sensitive film [71].

4.3 Multiple Luminescence Sensing Concepts

The detection of more than one luminescence signal simultaneously, and in some cases a combination of a luminescence and absorbance/reflectance determination, is very common and widely used in many sensor concepts[85]. Multiple sensing systems can come in various configurations and can be differentiated into two main formats: (i) multiple sensing using a single sensor and (ii) multiple sensing using more than one sensor parallel (see Figure 18). In comparison to a single luminescence signal measurement (intensity or lifetime) both methods require a more complicated optical setup and instrumentation. At least, more than one optical filters and detectors are required to measure the wavelength changes, and some sensing systems need an additional excitation light source (e.g. dual excitation and dual emission). However, a multiple sensing concept offers the possibility to measure multiple analytes at the same time. Examples are the simultaneous measurement of temperature and oxygen, or even of three parameters (pH, temperature and oxygen) [85]. Further, a reference dye can be added to reduce system drift or compensate the effect of other parameters affecting the sensing material (e.g. temperature).

The simplest configuration of such a sensor design is based on an array of multiple sensing spots or coated optical fibers sensitive to different analytes and aligned such as each sensor is in contact with the sample [32, 67, 86]. The effort for the instrumentation is relative high since the individual sensors typically need a separate optical path (if not using a camera) and the resolution is limited due to the distance between each sensor spot. Optical multi-sensors, having more than one indicator immobilized in the supporting matrix (single or multi-layer), are preferred since these enable a

simultaneous measurement of analytes directly at the same point [87–90]. Further, the use of a single sensor material with two indicator incorporated can be used for compensation methods. For example, oxygen sensors always show interference from temperature and incorporate a temperature-sensitive indicator which can compensate this effect. In addition, a reference dye can be added to compensate system drift and reduce bleaching effects and with a ratiometric approach it is possible to increase the signal-to-noise ratio and thus the resolution of the sensor.

Instead of measuring the luminescence intensity other multiple sensing methods used are based on the detection of luminescence lifetime. Two very popular techniques are the dual lifetime referencing (DLR) and dual lifetime determination (DLD). In both schemes the lifetime of two indicators are measured and the additional signal used for reference (see Section 4.3.1) or to determine a second analyte concentration (see Section 4.3.2). However, the following sections will give a detailed description of both methods and discuss advantages and disadvantages of multiple-lifetime measurements.
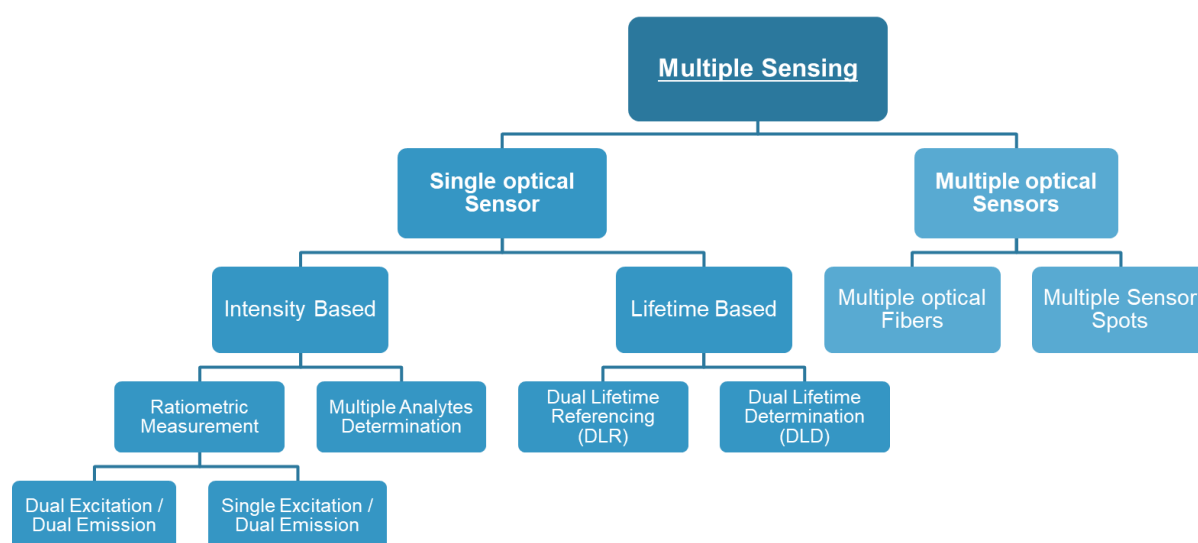

Figure 18: Block diagram of the different multiple sensing concepts and techniques.

4.3.1 Dual Lifetime Referencing (DLR)

In the Dual Lifetime Referencing (DLR) method a luminophore with a relative long decay time (typically in the µs region) is added as reference dye to a short-lived fluorescence indicator (decay time typically in the ns region) that is sensitive to the analyte [48, 91]. Both indicators require an overlap of absorbance and emission spectra to allow the excitation to occur with a single light source and the ratio can be determined in the time domain or frequency domain (see Figure 19). In the time domain scheme the reference dye and indicator are excited by a square pulse of light (see Figure 19A) and the overlapping emission of both measured in the first gate (A_1) whereas the slowly decaying phosphorescence reference dye is detected only when the light source is switched off (gate A_2) and when the analyte-sensitive indicator signal already has decayed. In the frequency domain method, both indicators are excited with a sinusoidal modulated light (see Figure 19B) and the measured signal ("total signal") is composed of the emission of the indicator that is affected by the analyte and the reference dye. However, a mathematical description of both methods can be found in the literature [48] and, in addition, the DLR technique is applied in many commercial sensing systems (see Section 6).
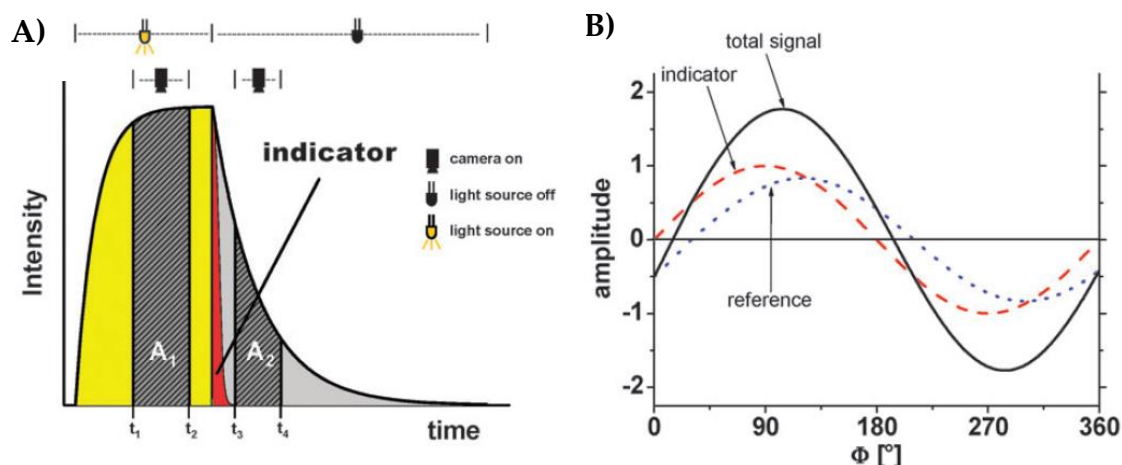
Figure 19: Schematic representation of the Dual Lifetime Referencing (DLR) in time domain (**A**) and frequency domain method (**B**) [85].

4.3.2 Dual Lifetime Determination (DLD)

The Dual Lifetime Determination (DLD) enables the simultaneous sensing of two or more parameters by separate the signals depending on their lifetimes only. Examples being the dual sensing of temperature and O_2 [92], pH and O_2 [89] as well as temperature and pressure [88, 93]. This method can be described as an extended scheme of the RLD technique (see Section 4.2), where the luminescence decay time of a second indicator is measured with two additional gates, A_3 and A_4 (see Figure 20). However, this method is only applicable if the luminescence decay times of both indicators are different by a factor of minimum 10, to achieve an efficient separation that is required.
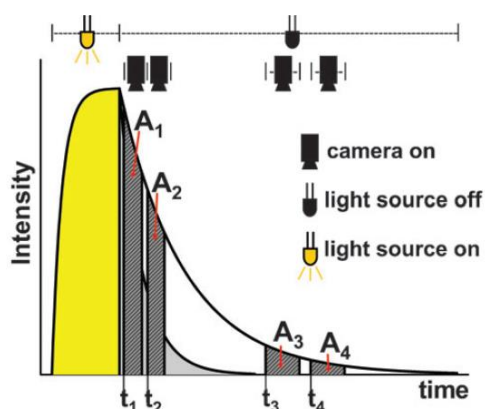
Figure 20: Schematic representation of the Dual Lifetime Determination technique (DLD) for a simultaneous sensing of two or more parameters [85].

4.3.3 Strengths and Weaknesses of these different measurement approaches

It is clear that the wide variety of different, indeed multiple sensing concepts and techniques would not have arisen had it not been for the various strengths and weaknesses each demonstrated, used as a route to optimization of the design. These may have been as a result of the state-of-the-art of the technology at the time (for example the state of development of different types of light sources such as LEDs and lasers), the ability to module these (either directly in the case of LEDs or diode lasers ot using different types of external modulator) and the availability of signal processing and

data processing software. Whilst such an analysis could be seen as somewhat subjective, Table 1 below presents the major strengths and weaknesses of the techniques seen in Figure 18.

Table 1: Major strengths and weaknesses of different measurement techniques [15, 94].

Technique	Key strength	Weakness
luminescence intensity	no complex chemistry required (only one dye); low-cost instrumentation (less complex optics and electronics required);	significantly influenced by instrument drift, dye bleaching & leaching and optical misalignment; interference from stray-light and temperature effects seen
luminescence decay time	precise; no complex chemistry required (only one dye); self-referenced (efficient compensation of dye bleaching & leaching); significantly less influenced by instrument drift, optical misalignment and stray-light	relatively expensive instrumentation; requires dyes with long luminescence life times, interference from temperature effects
two-wavelength referencing (ratiometric)	high precision, moderate influence from instrument drift, efficient compensation of optical misalignment, partial compensation of temperature	complex chemistry required (two dyes); complex & expensive instrumentation; photodecomposition, leaching and bleaching of the dyes may be different for each dye affecting calibration
dual lifetime referencing (DLR)	high precision; self-referenced; efficient compensation of dye bleaching & leaching, instrument drift, optical misalignment and stray-light; partial compensation of temperature	relatively expensive instrumentation; appropriate selection of two dyes required (different excited state of luminescence life times); more complex chemistry used

5   Optical Sensing Formats/Platforms for Optical O_2 and pH Sensors

A key parameter of absorption- and luminescence-based sensors is the optical platform that acts as interface between the analyte sensitive material and the optoelectronic components since the sensor performance strongly is linked to the platform design. Current trends are influenced by an increasing demand of such sensors in commercial applications and thus, new developments address the need of miniaturization, low-cost, repeatability, long-term stability and compatibility with mass-production methods. The sensor designs can be separated into two main groups: planar and fiber-optic formats. Planar sensing films are widely used and can be prepared at low cost. These films may be applied as sensor spots for "contactless" sensing of O_2 or pH [95, 96], can be designed for flow cell concepts [65, 67, 97–99], integrated into sensor caps [100] or sensing systems [64] (also see Section 6), as well as 3D-bioprinted constructions are possible [101]. However, this section will present an overview of platform designs developed in the past decade with a focus on fiber-optic concepts as well as fiber manipulation techniques and coating methods of optical fibers.

5.1 Fiber-Optic Sensor Designs

Optical fibers for luminescence-based sensors can be used in different configurations such as tip-based designs with a sensor material attached or doped cladding concepts to measure an evanescent field interaction. A huge amount of optical fibers are available now having different mechanical and

light-guidance properties [102–106] which have to carefully selected according to sensing technology and field of applications. Important parameters are the numerical aperture, the fiber size (diameter) as well as the materials of which the fibers are made up (e.g.: all-silica, polymer or a combination of both) since these influence the optical properties significantly [107–110]. Compared to all-silica fibers, PMMA-based polymer fibers typically have a higher numerical aperture, are highly flexible, thus are available with larger diameters (up to 3 mm), but have low light transmission below 350 nm and are not compatible with high temperatures [106, 111, 112].

A very common and successfully used sensor design has been based on a fiber tip that is tapered down to diameters smaller < one half of the fiber diameter during a thermal or chemical process [31, 32, 80, 81, 113–115] (commercial products: see Section 6). Tip diameters of < 50 µm are possible and results in very small sized sensor tips with fast response times because thinner coatings allows a faster diffusion of the analyte. In the literature [116], the authors shared preliminary results of fiber-optic pH and O_2 sensors based on a special tapered tip design. The sensors showed very fast response times of $t_{90} < 200$ ms for O_2 changes and $t_{90} < 3$ seconds for pH changes, as well as good long-term stability and high accuracy. Chipman et al. had developed a very fast tapered O_2 sensor and integrated it into a set-up specially designed for eddy correlation measurements in aquatic systems [10]. The tapered tip was coated with a thin (~20 µm) O_2 sensitive material based on ruthenium (II)-tris-4, 7- diphenyl-1, 10-phenanthroline perchlorate and thus the response time was fast (162 ± 66 ms) enough to detect O_2 fluctuations in a field test. The authors in [114] describe a chemical fabrication process to generate a cone shaped fiber-optic pH sensor. During the chemical taper process a multi-mode all-silica fiber (core/cladding: 50µm/125µm) was placed in a container with hydrofluoric acid (HF) (25% concentration) at the bottom and silicon oil above as protective layer (see Figure 21). After 40 minutes of etching the fiber was removed, cleaned and the cone shaped tip then coated with a pH sensitive layer using a dip coating process. The pH-sensitive material consists of three dyes (chlorophenol red, bromothymol blue and cresol red) sensitive for different pH values to receive an enhanced detection range from pH 4 to pH 11. Finally, with an additional thin film of TiO_2 (see Figure 21) the sensor showed a good stability and a relative fast response time of ~ 25 seconds. Others have used a comparable chemical process to etch a concave recess into the tip of a multi-mode fiber by removing parts of the core and then incorporated an O_2 sensitive polymeric material [117]. Other popular fiber-optic sensor designs have been based on an angled tips that are coated with a luminescence material and have the advantage to reduce the amount of excitation light that is reflected back to the detector. Examples are the O_2 sensors commercially available at Ocean Insight Inc. (details are given in Section 6).
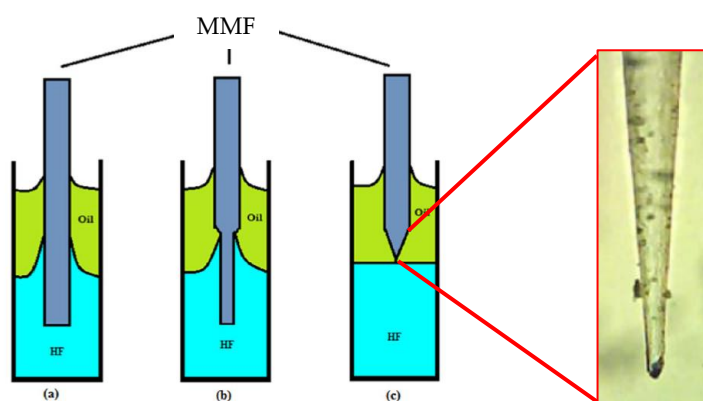

Figure 21: Schematic drawing of a chemical etching process to fabrication of a cone shaped fiber-optic pH sensor using HF (blue) and silicon oil (green). The tip is coated with a pH sensitive material and an additional thin film of TiO_2 (red) [114].

Another approach to attach a luminescence material at the tip of an optical fiber has through a photo-polymerization process. Mohamad et al. have used a multi-mode and multi-core fiber and employed such a method for developing a pH sensor [59]. The fiber used was based on 19 germanium-doped cores surrounded by a pure silica cladding. In such a device, first, the sensor side was chemically etched with HF to locally remove the cores and form a cavity on the tip and then placed into a solution containing a pH sensitive indicator (fluorescein O-methacrylate) as well as a photo-initiator and additional chemistry to run polymerization using a 405 nm laser. By coupling the laser light into a single core of the fiber (see Figure 22), the group demonstrated the possibility to generate single sensing spots selectively which has the potential to of fabricating a multi-analyte sensor.
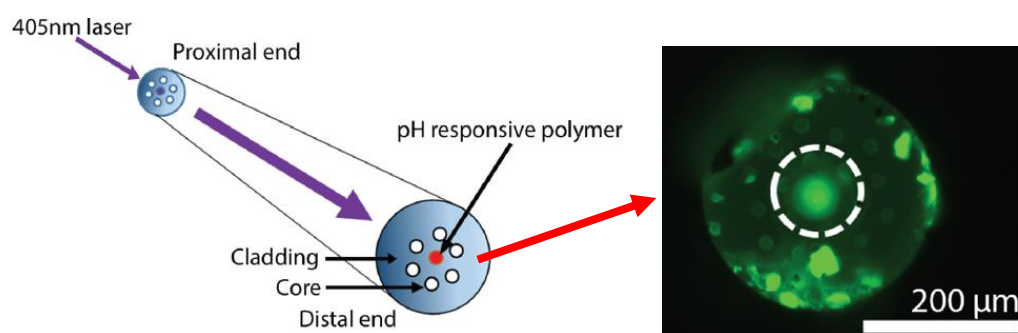

Figure 22: Schematic drawing of a photo-polymerization method to grow individual sensor spots at the end of a multi-core fiber using a 405 nm laser [59].

Zolkapli et al. have developed an O_2 sensor that was based on an evanescence wave sensing scheme using a polymer fiber [118]. Three small sections (~ 5 mm) of the cladding were removed along the fiber length during an etching process using acetone and each of the locations then was coated with a different luminophore-doped sol-gel (PtOEP, PdTFPP and Ru(dpp)$_3^{2+}$). This allowed the measurement of the O_2-dependent intensity changes of three luminescence materials simultaneously and thus to increase the dynamic range of the sensor. However, such a sensor was relative large but fabrication is simple, and thus suited for several possible applications. In addition, the measurement of an evanescence field interaction between the optical fiber core and a luminescence material attached to it was also successfully used in a fiber-optic flow cell sensors for the detection of O_2 [66] and pH [119]. Using the same physical effect, pH values may also be measured by using a single-mode fiber, where one side of the cladding was removed and then coated with a pH sensing membrane [120].The authors in further work [121] used a 3μm/125μm (core/cladding) single-mode fiber and removed parts of the cladding during a polishing process (see Figure 23). The side-polished fiber was then coated with a pH sensitive dye (methyl red, methyl orange, thymol blue, Nile red, or rhodamine-B) immobilized in a PVC matrix. The sensors thus fabricated were characterized using developed PWM-based sensing system and have a large dynamic range from pH 2 to pH 10, a very fast response time of about 8 seconds and a resolution of ~ 0.012 pH.
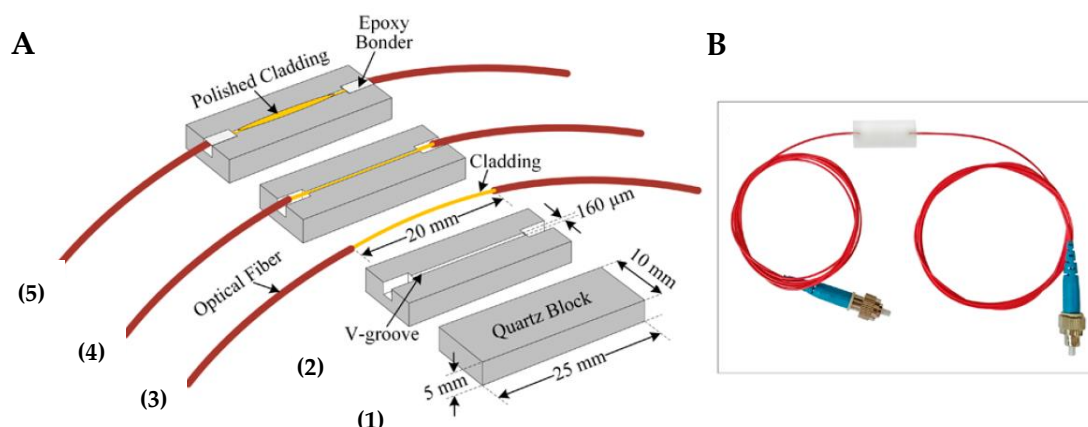
Figure 23: Schematic drawing of a polishing process (steps 1 to 5) to remove the cladding of a single-mode fiber (**A**) and photo of a side-polished pH sensor design (**B**) [121].

Other fiber-optic sensors developed have been based on special formed tips, like a U-bend structure (see Figure 24A) [122–124] or novel twisted-fiber designs (see Figure 24B). Chen et al. had developed a dual-core double-fiber [125] as well as a hexagonal 1-in-6 fiber [126] configuration pH sensors (see Figure 24B), fabricated by using a home-built twisting and gravitational-stretching system. A coaxial-twisting and gravitational-stretching procedure was utilized for optimal signal collection, to create minimal interference, and thus extreme small-sized probe tips with diameters between 2 μm and 70 μm were possible - these then were then coated with a pH sensitive dye (2',7'-bis(2-carboxyethyl)-5-(and-6)-carboxyfluorescein) covalently bound in a sol-gel. The very small tip, the relative fast response time of < 25 sec. and a biologically relevant pH range of pH 6.18 to pH 7.80 makes this sensor design ideal for intracellular single-cell pH measurement, which the group demonstrated in detecting single human lung cancer A549.
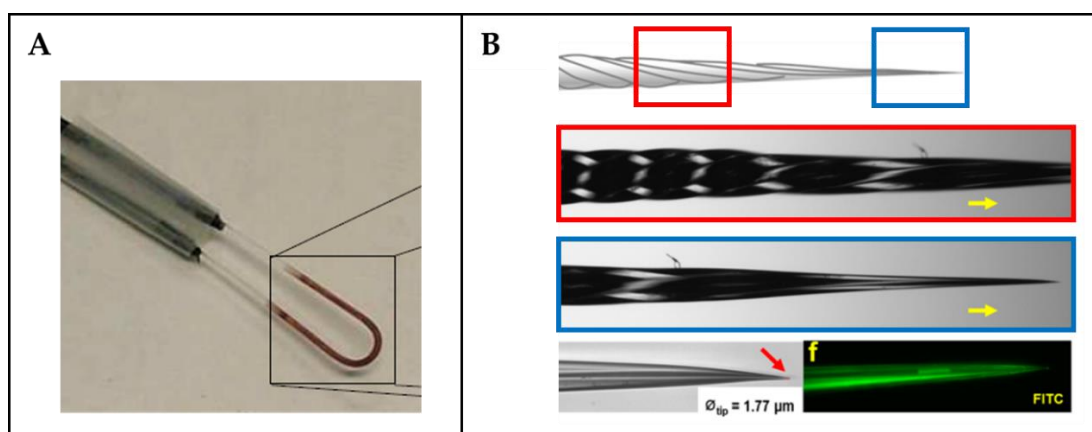
Figure 24: Photo of U-bend fiber-optic pH sensor with a Neutral Red nano-film coating (**A**) [123]. **B**: Schematic drawing of a twisted-fiber configuration with microscope images showing the center (red) and tip (blue) region as well as the fluorescence emission on the sensor tip [126].

5.2 Calibration of optical pH Sensors

The calibration of optical pH sensors varies from case to case, but a review of the literature shows that the most common approach is either to use buffer solutions (which can be purchased commercially) of known and fixed pH and then record the response of the sensor to being put into a container with such a solution, once a stable reading has been obtained [19, 127–130]. The sensor can then be cleaned (using deionized water) and then inserted in a further buffer solution – repeating this process until a calibration over the full range has been obtained. Often, however, new sensor designs

(such as fiber optic sensors) are calibrated with respect to a well-known commercial pH meter [128, 129], such as the glass electrode, when used in situations such as in the laboratory where its performance can be stabilized.

In some cases, authors claim a very high level of precision in the pH measurement, which clearly could only be obtained with a calibration against an instrument or buffer solution which has an equal (or indeed better) precision. Thus when claims, for example of a resolution of < 0.01 pH unit are made in the literature, unless the reader is skeptical of the result, this is only possible with carefully controlled laboratory conditions e.g. a fixed temperature and uncontaminated buffer solutions, representing the 'gold standard' for such calibrations, which then should be repeated regularly and systematically to maintain the quality of the calibration.

5.3 Calibration of optical O_2 Sensors

In general, optical O_2 sensors only require a two-point calibration: in an oxygen-free environment and in a known O_2 concentration. Typically 20.9% of O_2 is used as reference point since this allows a relative simple calibration in an air-saturated environment [131]. A common and conventional procedure to calibrate fiber-optic O_2 sensors is to operate the sensor in a 0% O_2 concentration using a nitrogen-saturated atmosphere or oxygen-free water (sodium sulfite solution) to obtain the first calibration point. The sensor is then dipped into air-saturated water or water vapor-saturated air to create the second measurement point at 20.9% O_2. A common procedure to prepare both calibration standards is described in the manufacturer's literature [131].

However, if very precise measurements of O_2 are required or for sensor characterization, a full multi-point calibration under carefully controlled laboratory conditions (e.g. temperature and pressure regulated) is necessary. A very common and often used method described in literature [64, 66, 132] is to place the sensor into a closed chamber that is filled with different ratios of O_2 and nitrogen gas. Using two gas flow regulators for O_2 and nitrogen, different and very precise O_2 concentrations can be passed through the chamber. To maintain a maximum accuracy of the calibration, the procedure then can be repeated regularly and systematically.

6   Commercial Developments of O_2 and pH Systems

A large number of commercial products offering different designs are available now and new innovative sensing materials, optical concepts and readout devices reported as a result increase the field of potential applications. In addition, new developments in optical components, electronics and detectors reduce the overall costs and enable miniaturized sensing systems to be envisaged which can detect single or multiple analytes (e.g. pH, O_2, pCO_2 and temperature) optically. In this section, the state of the art in commercial products in this field of luminescence-based sensors and instrumentation is discussed, with the focus on the comparison and evaluation of the different set-ups and sensor designs reported, considering also their flexibility and the breadth of their different fields of applications that result.

6.1 Commercially Available Sensors

The most commonly reported and thus widely used sensor designs are based on optical fibers with a sensing material attached to the distal end or tip. Due to their small size and the flexibility in positioning that is available, theses compact sensors are ideal for applications in biomedical, biological and healthcare-based research.

It would appear that the first commercially available fiber optical O_2 sensors were introduced by PreSens Precision Sensing GmbH (see Figure 25) and these are still available in different housings (e.g. NTH-PSt1, PM-PSt1 and FTCH-PSt1). The PSt1-Series typically is build-up of a silicate fiber with a diameter of 100 μm/140 μm (core/cladding) and they can be obtained with a flat tip (fiber cleaved)

or a tapered tip version. The taper was realized by heating and pulling the fiber with the goal of decreasing the fiber diameter to < 50µm (see Figure 26B). Then the fiber tips were coated with an O_2 sensitive dye (e.g. Ru(dpp), PtPFPP and PdTFPP) that was immobilized in a polymeric matrix (e.g.: polystyrene [31, 61] and ethyl cellulose), this being done by performing a simple dip coating process. A detailed description of patented coating mixtures can be found in [133, 134]. An additional coating, such as a black layer of silicone, can be attached in a second dip coating process that acts as optical isolation barrier, to reduce the influence of ambient light or auto-fluorescence of the sample [31]. Due to the materials used, the fiber tip typically is excited with green light, such as at a wavelength of 505 nm, and shows an emission in the red region (around 650 nm). In addition, the used indicator has a relatively long luminescence lifetime and thus is ideal for the preferred fluorescence-domain method (see Section 4.2), allowing low modulation frequencies in the sub-kHz region.

These sensors are suitable for the detection range of $0 - 50\%$ O_2, have a good accuracy of ± 0.4 % O_2 (determined at 20.9% O_2), are stable in the long-term and their calibration is relative simple (only 2 points are required). Further, with a tapered tip, it is possible to generate extremely small sensing tips with a reduced amount of coating material attached and this leads to a significantly faster response time (t_{90} < 3 sec. in gas phase) compared to the flat tip design (t_{90} < 30 sec. in gas phase). In addition, the same type of sensor designs are available for fiber-optic pH sensors (e.g.: NTH-HP5, PreSens Precision Sensing GmbH) based on the DLR (Dual-Life-Time Referencing) technique [48]. Here the coating comprises two indicators with different decay times but overlapping emission spectra, where one is dependent on the value of pH (e.g.: HPTS and fluorescein) and the other is independent (e.g.: transition metal complexes with ruthenium(II) or rhenium (I), phosphorescent porphyrins with platinum or palladium) of pH [135, 136]. These physically very small pH sensors have a detection range from pH 5.5 to pH 8.5, a good accuracy of ± 0.1 pH (determined at pH 7), a response time of t_{90} < 30 sec and are stable in the long-term. The sensors are pre-calibrated, however, for the best sensor performance the manufacturer recommends a multi-point-calibration prior to each measurement with five known buffer solutions.

Figure 25: Examples of commercial available fiber-optic O_2 sensor designs developed by PreSens Precision Sensing GmbH showing a PM-PSt1 needle type sensor (left) [131] and a FTCH-PSt1 flow through cell (right) [137].
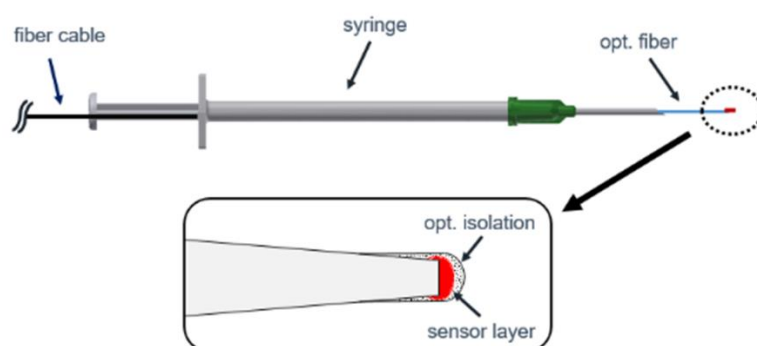
Figure 26: Schematic drawing of a fiber-optic O_2 microsensor with a syringe design and a tapered tip coated with an O_2 - sensitive layer and an over-coating of a black silicone for optical isolation [31].

Other sensors are available and designed to be particularly usable for monitoring in harsh environments. Examples are the O_2 sensing probes available from Ocean Insight Inc. (formerly Ocean Optics Inc.), where the optical fibers are glued in a stainless steel tubing and thus mechanically robust and protected in this way. These sensor are manufactured in different sizes (e.g.: fiber diameter and length) and have an angled tip coated with the O_2 sensitive layer (see Figure 27). The patent sensing membrane [138] consists of O_2 sensitive indicators, based typically on platinum complexes, like Pt(II) Octaethylporphin and Pt(II) meso-Tetra (pentafluorophenyl) that are immobilized in a hydrophobic sol-gel matrix. However, other sensors that are available are based on Ruthenium complexes, like the FOXY and HIOXY sensor series. The O_2 sensitive materials can be excited with blue light (e.g.: 380 nm or 475 nm) modulated between 2 kHz and 100 kHz (for luminescence-based lifetime measurements) and have an emission at wavelengths around 600 nm. The sensors have a very high sensitivity especially in the low O_2 range (0 – 5%) and, because of the very thin coatings, a relative fast response time of $t_{90} \approx 1$ second (see Figure 28). Further, the angled tip reduces the amount of excitation light that is reflected back to the detector which is an advantage compared to other tip designs. However, other companies also offer such robust O_2 probes with comparable designs (e.g.: PreSens Precision Sensing GmbH, PyroScience GmbH and Unisense).

Various Oxygen Sensor Probes

Figure 27: Various robust oxygen sensor probes with a stainless steel tubing (left) developed by Ocean Insight Inc. and an angled sensor tip of a FOXY-R sensor probe (right) [139].
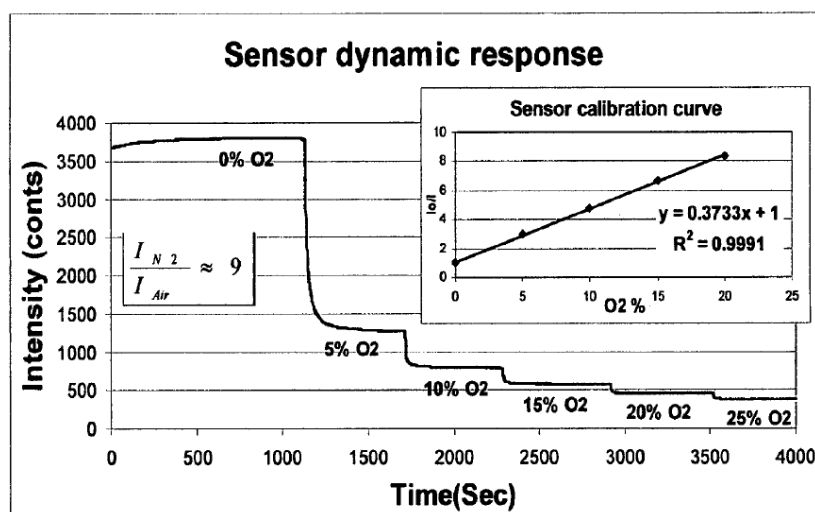
Figure 28: Sensor performance and calibration curve of a sol-gel based optical O_2 sensor developed by Ocean Insight Inc. when excited with 380 nm and measured at 645 nm [138].

The trend in commercial products seems to be shifting towards sensors with luminescence indicators for the near infrared region (NIR) and small sized and standalone systems with wireless communication that are also usable in harsh environments. Novel NIR indicators for the sensing of pH [140–142], O_2 [143, 144] as well as temperature [145] and carbon dioxide [146] are now available and some of these have been applied broadly in new commercial sensors, reported in particular during the last decade. Examples of these are platinum(II) and palladium(II) complexes with fluorinated benzoporphyrins that show excellent brightness in the NIR, longer luminescence lifetimes and improved photo-stability compared to other commonly used O_2 indicators (e.g. PtTFPP and Ru-dpp) [147]. Due to the very high luminescence brightness coatings can be prepared to be much thinner than in other sensors and therefore offer significant faster response times which then are possible (below 1 second).

A broad spectrum of commercial sensors (O_2, pH and temperature) based on such indicators are available now and they range from very small tapered tips (retractable or fixed designs) to robust fiber-optic designs (e.g. stainless steel housings) as well as replaceable sensor caps. Several examples are shown in Figure 29. The product line of PyroScience GmbH includes various fiber-optic based sensors that exist using optical fibers with diameters of 230 μm and tapered tips of 50 - 70 μm (e.g.: OXR50-UHS microsensors) as well as minisensors using optical fibers having diameters of 430 μm directly coated with a O_2 sensitive layer (e.g. OXF1100 minisensor). These sensors show faster response times of $t_{90} < 0.3$ to $t_{90} < 2.0$ s in the gas phase (depending on the fiber design and coating materials), have optimum detection ranges from 0 to 50% O_2 and an improved accuracy of ±0.2% O_2 (at 20% O_2). However, other versions optimized for a detection range of 0 - 10% O_2 are available as well. The oxygen sensitive coatings are excitable with red light (610 - 630 nm) and show an oxygen-dependent luminescence intensity and luminescence lifetime in the NIR region (760 - 790 nm), where excitation by light in the red region is preferred to reduce the effect of auto-fluorescence especially when using the sensors in biological applications. Further, the sensors come pre-calibrated for normal use: however, for more accurate measurements a 1 or 2-point calibration is recommended. Other sensor concepts, such as seen in the sensors from Unisense (see Figure 29C), are equipped with E^2PROMs (mono audio connector) that are readable with their instruments, having unique sensor identifications available and offer a user-friendly calibration retrieval.

A very innovative sensing concept is based on replaceable sensor caps available from PyroScience GmbH (see Figure 29D), these being specially developed for underwater applications [148] and these are usable with various the recently developed instruments (see Section 6.2). The caps have an optical fiber in them that is coated with an O_2-sensitive layer and are mechanically protected by the housing. Further, the replaceable caps are available for different detection ranges and with response times comparable to the already introduced fiber-optic sensors. The inventors in [149] describe a comparable design of sensors caps for the sensing of O_2, SO_2, H_2O_2, and pCO_2.
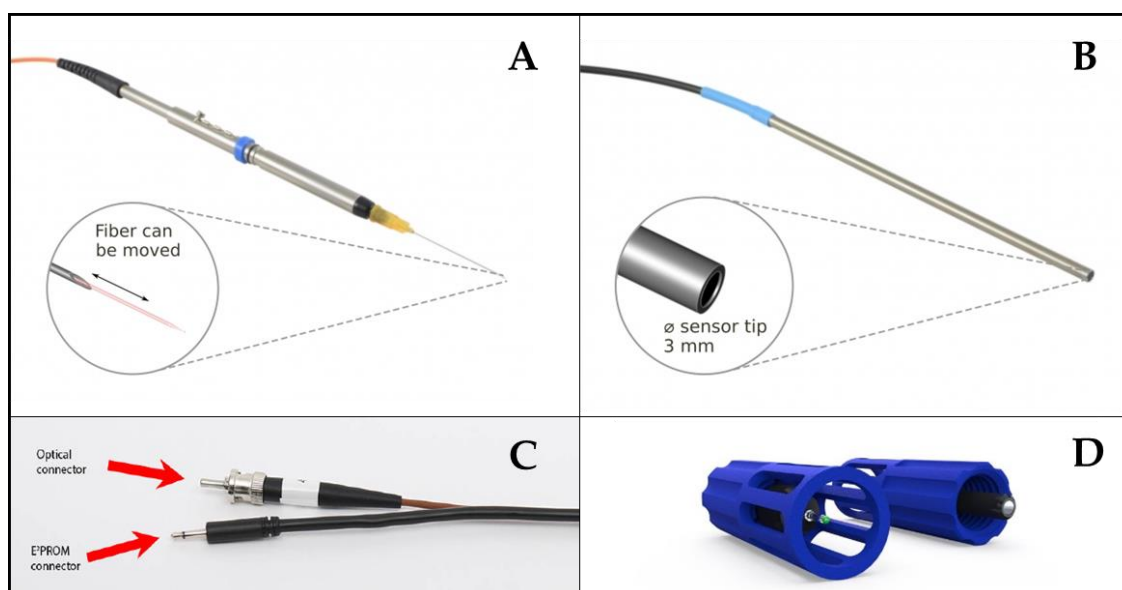
Figure 29: Examples of commercial available O_2 sensors based on novel NIR indicators. **A**: Retractable microsensor with a tapered tip and very fast response time of t_{90} < 0.3 sec. (OXR50-UHS, PyroScience GmbH) [150]. **B**: Robust sensor design with a fiber-optic O_2 sensor protected in a stainless steel tubing (OXROB10, PyroScience GmbH) [151]. **C**: Fiber-optic O_2 sensor equipped with an E^2PROMs for unique sensor identification and calibration retrieval (Unisense) [152]. **D**: Replaceable sensor caps with a protected fiber-optic O_2 sensor in it (PyroScience GmbH) [148].

Robust fiber-optic pH sensors based on replaceable sensor caps are commercially available from PyroScience GmbH (see Figure 30A) - these are sensitive to a pH range of 2-3 pH units, have response times of t_{90} < 60 sec., an accuracy of ±0.05 pH and are stable in the long-term. Compared to other luminescence based pH sensors, only a 2-point calibration is required. The pH sensitive coatings typically exists with aza-BODIPY dyes [153, 154] that show bright luminescence emissions in the NIR and pKa values can be tuned in a wide range [140, 141]. Further, by adding an appropriate reference indicator, pH sensing using a ratiometric approach or the DLR technique is possible [140]. Here, both indicators are excited with red light and the luminescence intensities or phase shifts (NIR) are measured at the same. Figure 31 shows the spectral properties of such a dual-lifetime referenced sensor and the pH response after calibration. Comparable coating materials and similar optical concepts are used in the pH sensors and pH instruments (see Section 6.2) available from PyroScience GmbH.

Further, sensor spots are available suitable for a "contactless" detection of pH, O_2 as well as temperature of samples in closed containers (see Figure 30B) where an optical fiber is used to guide the excitation light to the patch and emission light back to the detector.
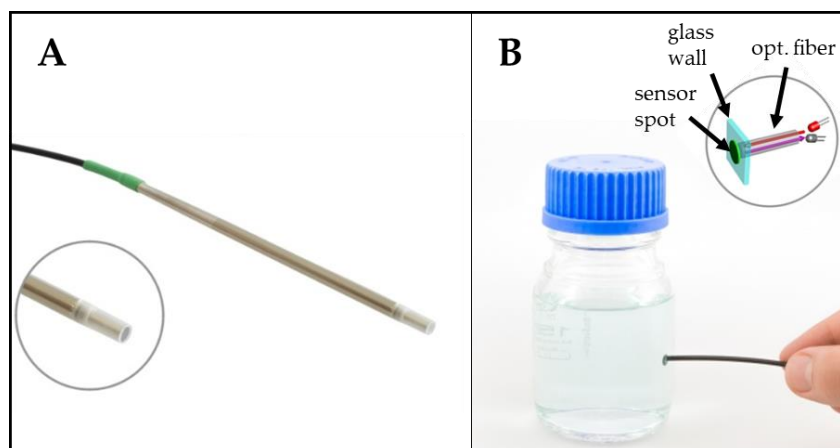
Figure 30: Examples of commercial available pH sensors based on novel NIR indicators. **A**: Robust fiber-optic sensor based on replaceable sensor caps with response times of $t_{90} < 60$ sec. (PHROBSC-series, PyroScience GmbH) [130]. **B**: Sensor spots for "contactless" sensing of pH; also available for detection of O_2 and temperature, with a sensor spot inside a closed glass bottle (PyroScience GmbH) [155].
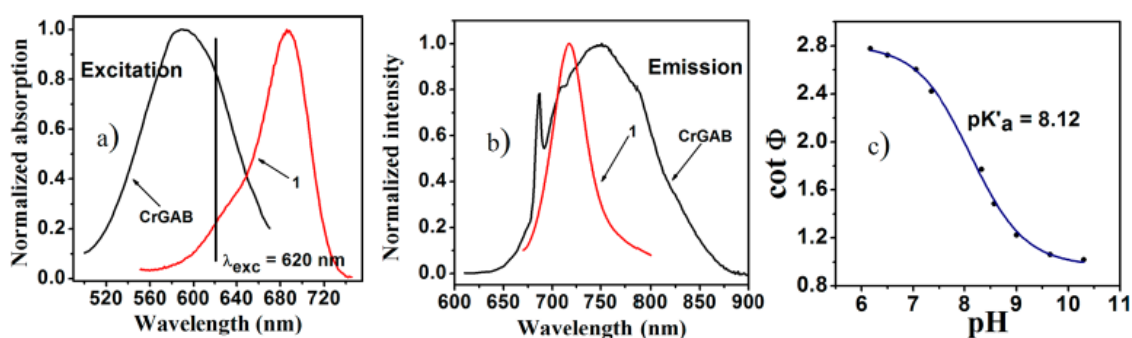

Figure 31: Spectral properties of a pH sensitive luminescence material for NIR. **A**: Excitation spectrum of the reference (black) and pH sensitive indicator (red) in protonated form. **B**: Emission spectra of both indicators when excited at 620 nm. **C**: Calibration result of a dual-lifetime referenced sensor with reference and pH indicator immobilized in hydrogel D4 [140].

6.2 *Commercially Available Instruments and Sensing Systems (OEM Solutions)*

In the last decade a growing number of sensing systems have been developed and became commercial products. Due to new technologies available now, such instrumentations range from very robust designs for harsh environments, like deep water and explosion hazard areas, to very compact and standalone concepts that are battery powered and equipped with a wireless communication (e.g.: Bluetooth). Further, some novel systems now offer a higher user flexibility and are available for the detection multiple analytes (e.g.: pH, O_2 and temperature) with a single instrument.

One of the first commercially available instrument for luminescence lifetime-based O_2 sensors based on the frequency-domain method is the Microx TX3 device (formerly OxyMicro) [156] from PreSens Precision Sensing GmbH. The optical set-up and operating mode is comparable to that shown in Figure 15 and described in Section 4.2. Further, it can be equipped with a temperature sensor (Pt100) for additional measurement and compensation purposes. The optics is optimized for fiber-optic based sensors with typical diameters of 100μm/140μm (core/cladding) and O_2 sensitive dyes for excitation wavelengths in the green region (e.g.: 505nm) and red emission (e.g.: 650nm), like the PSt1-Series from PreSens Precision Sensing GmbH (see Section 6.1). However, these kind of instruments are also available as multi-channel versions in order to connect more than one fiber-optic

O_2 sensor, ideal for fine-scale measurements of oxygen distribution [81]. In addition, PreSens Precision Sensing GmbH offers a commercially available instrumentation for their fiber-optic pH sensors (see Section 6.3). The optical set-up is comparable to that used in the Microx TX3 (see Figure 15) but based on the in 2003 patented [135] DLR technique [48, 94]. Here the pH sensitive coating is excited with a blue light (typically around 470 nm) and decay times of the emission light (between 520 nm and 650 nm) of two indicators are measured. Since both indicators, the one that is dependent to pH and the other that is independent to pH, have relatively long decay times in the µs region, the excitation LED can be sinusoidal modulated in with frequencies in the low kHz range (e.g.: 80 kHz).

Another detection system for fiber-optic sensing concepts is shown in [157] (see Figure 32) and a comparable instrument is commercially available from Ocean Sight Inc. (see Figure 33). A bifurcated fiber-bundle is used to guide the excitation light ($\lambda_{ex.} \approx 475$ nm) to the tip of a fiber-optic sensor (see Section 6.1: sensors from Ocean Insight Inc.) and a portion of the luminescence emission (here: $\lambda_{em.} \approx 600$ nm) is collected and guided through the other branch of the fiber-bundle back to a detector (spectrometer or photodetector). These bifurcated fiber-bundles are available in different diameters and typically are build-up of a large number of single optical fibers with diameters less than 40 µm. Figure 33 shows the end-face of a bifurcated cable (BIFBORO-1000-2, Ocean Insight Inc.) realized with ~500 single optical fibers. This optical set-up has the advantage to allow a connection of fiber-optic O_2 sensors with different diameters ranging from the very small (e.g. 100 µm) to the very large (e.g.: 1 mm) with a very good light coupling efficiency. Further, the light is modulated between 2 kHz and 100 kHz to offer a luminescence lifetime measurement that is used in the commercially available instrumentation (e.g.: NeoFox, Ocean Insight Inc.).
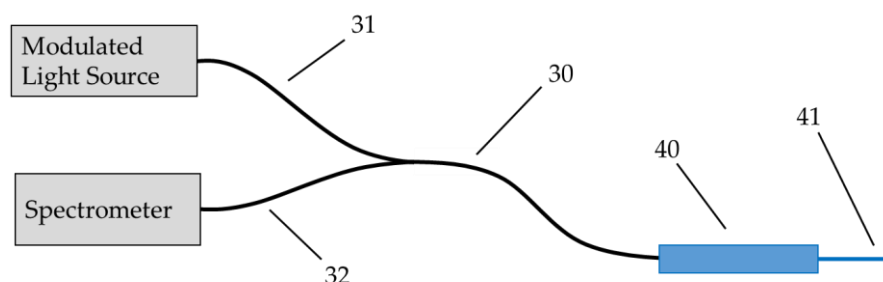

Figure 32: Schematic drawing of a detection system for fiber-optic O_2 sensors. 30: Bifurcated fiber-bundle (31: first branch; 32: second branch), 40: O_2 sensor, 41: tip coated with O_2 sensitive layer [157].
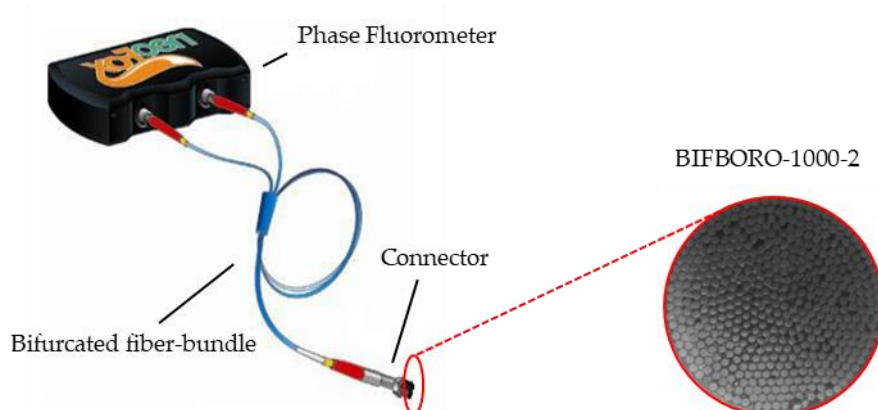

Figure 33: Set-up of a phase fluorometer system (NeoFox) [158] from Ocean Insight Inc. showing the end-face of a bifurcated fiber-bundle (BIFBORO-1000-2) [159].

However, since novel NIR indicators for O_2, pH and even temperature (see Section 6.1) became available, commercial developments in the last 5-10 years have mainly been focused on sensing system based on these. Companies like PyroScience GmbH, PreSens Precision Sensing GmbH and Unisense now offer a large number of different instruments and an expanded field of applications offered with their innovative products. An overview of devices for the optical sensing of pH, O_2 and temperature are shown in Figure 37. Because of the novel indicators, as well as the further developments in optical and electronical components, very small sized and long-term stable instrumentation is now available. A very compact and standalone sensing system for O_2 is available at PyroScience GmbH (see Figure 34) - one that can be powered and communicate via USB. Further, it offers a UART interface for a simple integration into external systems (OEM) [160]. The system is based on their "REDFLASH" technology (a name introduced by the company) and on their patented set-up [161] that reduces the effect of temperature during luminescence-based O_2 measurements significantly and increases the long-term stability (typical drift < 1% O_2/year at 21% O_2) and shelf life (typical > 5 years). The key feature is an optimized temperature insulation of the instrument (housing and internally) and of the O_2 sensitive layer (see Figure 34B). The O_2-sensitive coating (Figure 34B, #4) typically exists as a NIR indicator immobilized in a polymer (examples in Section 6.1) that allows an excitation with a low-cost red LED (Figure 34B, #2). In order to insulate the sensing layer from quick temperature changes in the analyte, an additional coating of a hydrophobic material, such as PTFE or PE, is added with a layer thickness between 0.5 mm to 2 mm (Figure 34B, #8). Further, the insulating layer has very small pores (sizes between 50 μm to 200 μm) to overcome convective heat exchange but still to allow the diffusion of the analyte (here O_2). In addition, the internal components, like optical filters, LED, detector and electronics are also thermally insulated (Figure 34B, #15). Since long-term and slow temperature changes might still affect the measurements, the inventors had attached a temperature sensor (Figure 34B, #5) to the housing and closed to the sensing element for compensation purpose. To allow a transmission of light between the sensing element and the internal optical parts the housing is covered with a transparent plastic (Figure 34B, #6) and equipped with a mounting thread for installation.
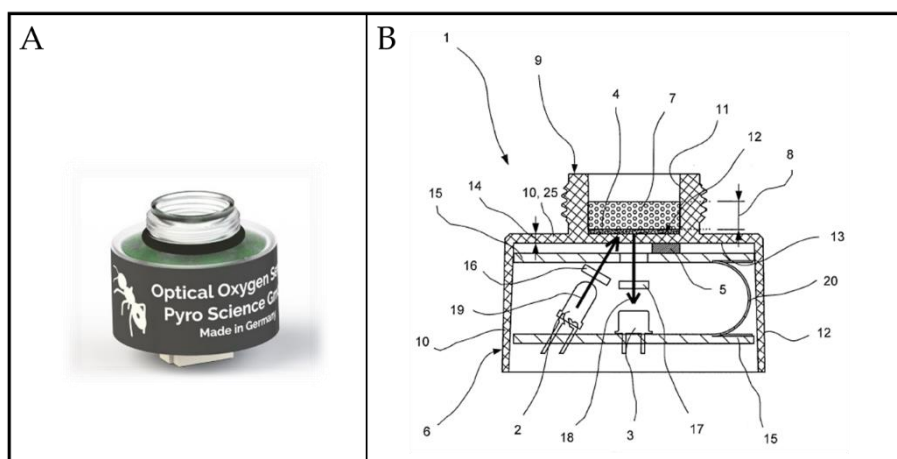
Figure 34: Image (**A**) and schematic drawing (**B**) of a commercially available O_2 sensing system (FDO2) from PyroScience GmbH with an optimized temperature insulation [160, 161].

PyroScience GmbH also offers a commercially available instrumentation developed for deep seawater analyzes down to 4000 m (see Figure 35A) [162]. The system is usable with sensor caps and fiber-optic sensors (see Section 6.1) for a luminescence-based sensing of O_2, pH or temperature in the NIR. The possibility to measure three parameters with one instrument is unique and offers a maximum flexibility for the users. However, a comparable detection system for the measurement of O_2, pH and pCO_2 has been described in the literature [129] (see Figure 35B). The instrument includes a compact phase fluorimeter for luminescence lifetime measurements in the NIR, and is equipped

with a temperature sensor (Pt100) for compensation purposes, being designed for autonomous long-term measurements (with a lithium battery and data logger included). Further, the authors describe the calibration procedure and compensation methods, and have characterized the whole system with respect to long-term stability, the effect of temperature and salinity. Figure 36 shows the materials used for the sensing layers, the spectral properties of each indicator and the calibration curves determined with the detection system. Finally, the set-up was successfully tested in different sea water applications.
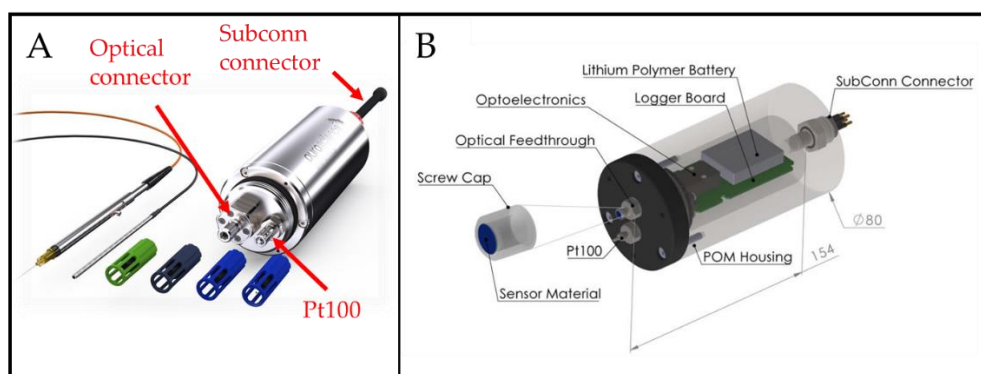
Figure 35: Image of a commercial instrumentation for deep seawater analyzes usable with sensor caps and fiber-optic sensors for O_2, pH and temperature (**A**) available at PyroScience GmbH. Sketch of a comparable system showing the electronic board, optoelectronic and battery in a pressure housing (**B**). Both systems are equipped with a Pt100 for temperature compensation [129, 162].
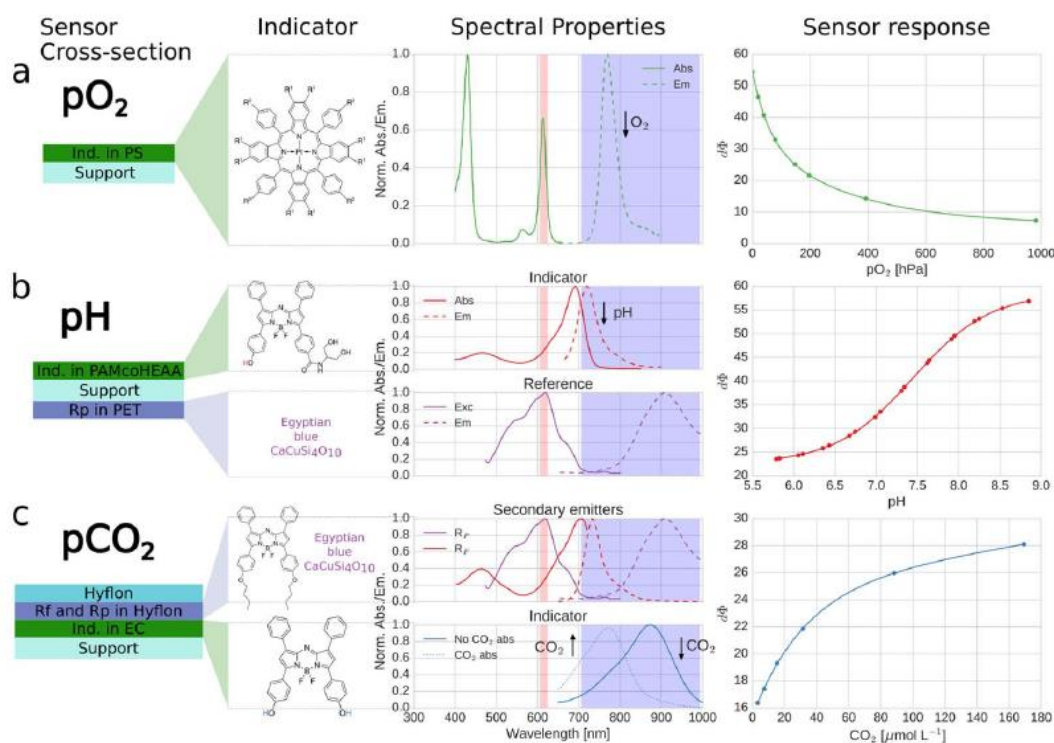
Figure 36: Schematic of the chemistry used for the sensing of O_2, pH and pCO_2 in sensor caps used with detection system in Figure 35B and shows the spectral properties (absorbance and emission) of the sensor designs as well as the excitation wavelengths (red area) and signal collecting wavelengths of the instrument (purple area) in the graphs. The sensor response shows the calibration curves determined with the system [129].

However, several other detection systems based on a comparable measurement technology for NIR optical sensors for the sensing of O_2, pH and temperature are available. Examples of such instrumentation, optimized for fiber-optic sensors use, are the FireSting pro (see Figure 37A) [163] from PyroScience GmbH, usable for multiple analytes (O_2, pH or temperature), and the OXY-1 ST (see Figure 37C) from PreSens Precision Sensing GmbH (for O_2 only) [164]. These are lightweight devices ideal for measurements in laboratory environments and are also available in multi-channel versions. Other detection systems available are very small-sized, powered and readable via a USB connector (or UART) and can be equipped with replaceable fiber-optic based O_2 sensors (see Figure 37B) [165–167]. Further, PreSens Precision Sensing GmbH developed a very compact and standalone O_2 meter (see Figure 37D) that is temperature compensated (internally), offers a wireless communication via Bluetooth and thus is controllable and readable with a smartphone or tablet [168]. Ideal for the monitoring of oxygen in packaging or sealed containers.
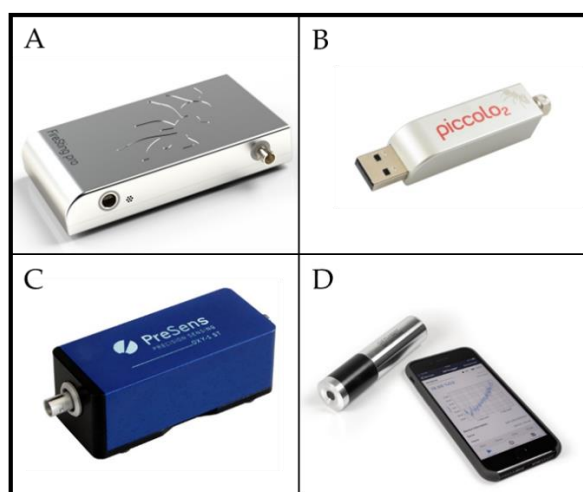
Figure 37: Overview of compact and lightweight detection systems for optical O_2, pH and temperature sensors. **A**: Firesting pro (PyroScience GmbH) [163], **B**: PICO2 (PyroScience GmbH) [167], **C**: OXY-1 ST (PreSens Precision Sensing GmbH) [164], **D**: OXYLogger (PreSens Precision Sensing GmbH) [168].

6.3 Comparison and Overview of Commercial Sensors and Instrumentations

To summarize and to allow a convenient cross-comparison, Table 2 - 4 gives an overview of commercially available luminescence-based sensors, instruments and sensing systems (OEM solutions) that are exemplary for the current state of technology in commercial products. All data shown are obtained from the manufacturer websites.

Table 2: Examples of commercially available O_2 Sensors. All data obtained from the manufacturer websites.

Manufacturer	Product (sensor type)	Housing & Sensor Size	Detection Range [A]	Resolution	Resp. Time t_{90}	Drift	Highlights / Features	Examples of Application Areas
PyroScience GmbH [150]	OXR50-UHS (fiber-optic)	needle-type ø = 50 - 70 μm	0 - 50% O_2	0.05% O_2 [B]	< 0.3 sec. (gas)	negligible	very small, very fast, negligible drift, long shelf life (> 3 years), retractable	micro-profiling in biological & environmental research, medical & life science research, fast applications
PyroScience GmbH [151]	OXROB10 (fiber-optic)	stainless steel ø = 3 mm	0 - 50% O_2	0.05% O_2 [B]	< 7 sec. (gas)	negligible	robust, negligible drift, long shelf life (> 3 years), very long lifetime (> 10 M data points)	process environments, biological research, environmental research
PyroScience GmbH [148]	OXCAPG-UHS-SUB (sensor cap)	special protective cap design	0 – 720 μmol/L (0 - 50% O_2)	± 0.8 μmol/L [E]	< 0.3 sec. (liquid)	< 2% in 3 months	robust, easily exchangeable, very fast, very low drift, special design for underwater applications	deep seawater analyzes, fast profiling (e.g.: eddy covariance measurements)
PreSens Precision Sensing GmbH [169]	PM-PSt8 (fiber-optic)	needle-type ø < 50 μm	0 - 10 % O_2	± 0.06% O_2 [C]	< 3 sec. (gas)	N/A	very small, long shelf life (> 5 years), high resolution in low O_2 concentrations, retractable	micro-profiling in biological & research, medical & life science research
PreSens Precision Sensing GmbH [170]	OIM-PSt6 (fiber-optic)	stainless steel fitting	0 - 5 % O_2	± 0.0015% O_2 [D]	< 6 sec. (gas)	< 2 ppb (within 30 days) [F]	robust, very high resolution, autoclavable, pressure resistant, low drift, long shelf life (> 5 years)	process control, bioreactors, in-line measurements (e.g.: brewing and beverage industry)
Ocean Insight Inc. [139]	FOXY-T1000 (fiber-optic)	stainless steel ferrule, ø = 6.35mm	0 - 100% O_2	0.05% % O_2	< 1 sec. (gas)	0.03 % O_2 per hour	robust, angled tip, fast, autoclavable, pressure resistant	process environments, high-pressure applications
Unisense [171]	Opto-430 Fast (fiber-optic)	needle-type ø = 430 μm	0 - 50% O_2	N/A	< 0.3 sec. (gas)	N/A	small, very fast, equipped with E²PROM for sensor ID & calibration data, retractable	biological & environmental research, medical & life science research, fast applications
World Precision Instruments Inc. [172]	O2-T0050L250-12011T (fiber-optic)	needle-type ø < 50 μm	0 - 50% O_2	< 0.09% O_2 [B]	< 3 sec. (gas)	< 0.1% (O_2 within 30 days) [F]	very small, integrated temperature sensor, usable with PreSens device, retractable	micro-profiling in biological & environmental research, medical & life science applications, physiological applications
World Precision Instruments Inc. [172]	O2-T0050L250-12021T (fiber-optic)	needle-type ø < 50 μm	0 - 50% O_2	< 0.09% O_2 [B]	< 3 sec. (gas)	< 0.1% (O_2 within 30 days) [F]	very small, integrated temperature sensor, usable with Ocean Insight device, retractable	

[A] optimum detection range, [B] determined at 20% O_2 (gas), [C] determined at 2.5% O_2 (gas), [D] determined at 0.2% O_2 (gas), [E] determined at 275 μmol/L, [F] sampling interval of 1 minute.

Table 3: Examples of commercially available pH, pCO$_2$ and temperature sensors. All data obtained from the manufacturer websites.

Manufacturer	Product (*sensor type*)	Housing & Sensor Size	Detection Range [A]	Resolution	Resp. Time t_{90}	Drift	Highlights / Features	Examples of Application Areas
PyroScience GmbH [130]	PHROBSC-PK6 (*pH: fiber-optic*)	stainless steel ø = 4 mm	pH 5.0 - 7.0	0.003 pH (at pH 6.0)	< 60 sec.	< 0.005 /day (at pH 6.0)	robust, exchangeable sensor caps, very low drift, high resolution	process environments, biological research, environmental research
PyroScience GmbH [173]	PHCAP-PK7-SUB (*pH sensor cap*)	special protective cap design	pH 6.0 - 8.0	0.003 pH (at pH 7.0)	< 60 sec.	< 0.005 /day (at pH 7.0)	robust, easily exchangeable, very low drift, high resolution , special design for underwater applications	biological research, environmental research, deep seawater analyzes
PreSens Precision Sensing GmbH [174]	PM-HP5 (*pH: fiber-optic*)	needle-type ø < 150 µm	pH 5.5 - 8.5	± 0.02 pH (at pH 7.0)	< 30 sec.	< 0.05 /day [B]	very small, good detection range, long shelf life (> 2 years), retractable	micro-profiling in biological research, medical & life science research
PreSens Precision Sensing GmbH [175]	FTC-SU-HP5-US (*pH flow cell*)	different T-cell volumes (0.3 - 8.3 mL)	pH 5.5 - 8.5	± 0.02 pH (at pH 7.0)	< 120 sec.	< 0.005 /day [B]	easy integration into perfusion systems, good long-term stability, good detection range	monitoring in bioreactors, online measurement in perfusion systems
PreSens Precision Sensing GmbH [176]	SP-HP5-SA (*pH patch*)	Different spot diameters available	pH 5.5 - 8.5	± 0.01 pH (at pH 7.0)	< 120 sec.	< 0.005 /day [B]	easy integration into transparent glass or plastic vessels (self-adhesive), good long-term stability, good detection range	monitoring in shake flasks, "contactless" measurements through transparent materials
World Precision Instruments Inc. [177]	PH-T0400L250-12021 (*pH: fiber-optic*)	needle-type ø < 100 µm	pH 5.5 - 8.5	± 0.02 pH (at pH 7.0)	< 5 sec.	< 0.05 pH/h [E]	very fast, very small, good detection range, retractable	micro-profiling in biological & environmental research, medical & life science research
PreSens Precision Sensing GmbH [178]	PM-CDM1 [C] (*pCO$_2$: fiber-optic*)	needle-type ø = 250 µm	0.04 - 5 % CO$_2$	± 0.1 % (at 1 % CO$_2$)	< 5 min. [D]	N/A	small, retractable	micro-profiling in liquids & semi-solid substrates, physiological applications
PyroScience GmbH [179]	TPR430 (*Temp: fiber-opt.*)	needle-type ø = 430 µm	0 - 50° C	0.02° C	< 0.1 sec. (liquid)	< 0.1° C /day	small, high resolution, very fast low drift, very long lifetime (> 10 M data points), long shelf life (> 3 years), retractable, works in gas and liquid	temperature compensation of optical sensors, micro-profiling applications

[A] *optimum detection range*, [B] *sampling interval of 1 minute*, [C] *prototype with preliminary specifications available*, [D] *for a CO$_2$ change from 0.5 to 1 %*, [E] *sampling interval of 1 second.*

Table 4: Examples of commercially available instrumentations for optical O₂, pH and temperature sensors as well as wireless sensing systems and OEM solutions.

Manufacturer	Product	Analyte	Sensor Type	Housing & Size	Highlights / Features	Examples of Application Areas
PreSens Precision Sensing GmbH [180]	OXYPro	O_2	sensing system (OEM solution)	stainless steel, ø = 12 mm, L = 120 - 420 mm	compact standalone device, standard PG 13.5 thread, exchangeable sensor caps (stainless steel), stands steam sterilization, integrated temperature sensor, pressure resistance, analog output	food applications, industrial processes, bioreactors, aggressive environments
PreSens Precision Sensing GmbH [168]	OXYLogger	O_2	wireless sensing system	stainless steel, ø = 28 mm, L = 116 mm	compact standalone device, robust, Bluetooth & smartphone app, battery powered (rechargeable), integrated temp. sensor, long shelf life (> 5 years)	monitoring in packaging & products
Unisense [181]	FOM Deep	O_2	fiber-optic micro-sensors	N/A	standalone device for water depth down to 4000m, fully submersible housing, integrated temperature sensor	biological research, environmental research, deep seawater analyzes, eddy covariance measurements
PyroScience GmbH [167]	PICO2	O_2	fiber-optic sensors, sensor patches	USB stick housing, 15 x 15 x 54 mm	very compact device, USB interface, low power consumption	high through-put screening, microfluidic applications, "contactless" measurements
PyroScience GmbH [160]	FDO2	O_2	sensing system (OEM solution)	standard form factor (M16x1, ø = 28 mm)	optimized temperature insulation and compensation, fast response (t_{63} < 2 sec.), low drift (< 1% O_2/year at 21%), integrated ambient pressure sensor, very long lifetime (> 50 M data points), long shelf life (> 5 years), UART interface	gas stream measurements, monitoring in incubators & inert gas processing chambers
PyroScience GmbH [163]	Firesting Pro	O_2, pH and Temp (opt.)	fiber-optic sensors	78x120x24 mm	multiple analytes, USB powered, connector for temp. sensor, integrated ambient pressure & pressure sensor, multi-channel versions available, analog output	laboratories, biological research, microfluidic applications, high through-put screening and more
PyroScience GmbH [162]	AquapHOx-LX	O_2, pH and Temp (opt.)	sensor caps	titanium, ø = 63 mm, L = 300 mm	standalone device for multiple analytes, exchangeable sensor caps, high pressure resistant (400 bar), operates up to 4000 m depth, USB powered, analog outputs	environmental research, deep seawater analyzes, eddy covariance measurements
PreSens Precision Sensing GmbH [182]	pH-1 SMA HP5	pH	fiber-optic sensors	95x34x30 mm	compact and lightweight, USB powered, connector for temp. sensor	laboratories, biological research, cell culturing
World Precision Instruments Inc. [177]	PH-LUX-PROT	pH	fiber-optic sensors	200x124x45 mm	compact and lightweight, Wifi & LAN integration, controllable with smartphone (or tablet) and PC, USB powered	laboratories, biological research, cell culturing

7 Summary, Future Prospects and Outlook for such Sensors

In this work, the aim has been to demonstrate that luminescence-based optical sensors, especially for the sensing of O_2 and pH, are at an advanced state and that sensing schemes as well as commercial developments have experienced a fast growth in the last decade. Highlighting the progress in optical O_2 sensors and sensing systems (standalone and OEM solutions), these type of sensors are in the process of replacing the classical Clark electrodes in many fields of applications. O_2 sensors based on NIR luminescence materials and optimized optical platforms have led to significant improvements in sensing performance and offering long-term stability. Commercial sensors are now very reliable and some are available with very fast response times (< 0.3 s), very small tip sizes (ø = 50 - 70 µm), long shelf life (> 5 years) and negligible drifts. In addition, the fact that companies have increased their product range for the optical sensing of O_2, pH as well as temperature and pCO_2 (see Section 6) shows the significance of the field and now products range from very small sensor designs, usable in biomedical applications, to very robust sensors as well as replaceable sensor cap concepts for harsh environments, such as industrial applications or deep seawater analyzes. Novel commercial instruments and standalone systems are often now very compact (e.g.: USB stick format), battery powered, usable for multiple analytes and some offer a wireless communication via smartphone/tablet and have been applied to numerous impressive applications (a highly topical example is the sensing system that was tested and integrated by NASA in the Mars Rover 2020).

It is always challenging to consider future prospects for the field but all the research effort and the rapid commercial developments seen in particular during the last decade provide evidence that the positive trends mentioned above will continue and, it is hoped, in the next 10 years more optical sensors will be created to replace conventional sensors. This will take advantage of the developments in the field which will support it – new optical sources which typically will be higher in power, wider in wavelength range (to open up the use of a wider range of indicators) and capable of easier, direct modulation. All this will be coupled to greater computing and thus signal processing power to analyze the outputs of the sensors and likely the development of new, more stable and better indicator dyes themselves which can most easily be incorporated into the sort of senor systems described.   This will likely allow sensing systems to become smaller and better suited to in-the-field use, and a reduction of production costs and the incorporation of the above new developments will open new, potentially large markets (e.g. single-use applications, lab-on-a-chip and wearable concepts).   The need for new, more versatile and cheaper sensors will support creating novel fiber-optic designs, using 3D-bioprinted, inexpensive elements. All this points in the direction of improvements in sensor performance (see Sections 5 & 6) which indicate that research in this area will move forward in many different directions, with new sensors finding the way to high volume production and thus to continue to enlarge the field of applications of this innovative technology. The future prospects in this field are excellent and will continue to be the subject of innovative research for many years to come.

References

[1]   S. Kojima and H. Suzuki, "A Micro Sensing System for Blood Gas Analysis Constructed With Stacked Modules," *IEEJ Trans. SM*, vol. 124, no. 4, pp. 111–116, 2004, doi: 10.1541/ieejsmas.124.111.

[2]   D. B. Papkovsky, N. Papkovskaia, A. Smyth, J. Kerry, and V. I. Ogurtsov, "Phosphorescent Sensor Approach for Non-Destructive Measurement of Oxygen in Packaged Foods: Optimisation of Disposable

Oxygen Sensors and their Characterization Over a Wide Temperature Range," *Analytical Letters*, vol. 33, no. 9, pp. 1755–1777, 2000, doi: 10.1080/00032710008543157.

[3]   A. S. Jeevarajan, S. Vani, T. D. Taylor, and M. M. Anderson, "Continuous pH monitoring in a perfused bioreactor system using an optical pH sensor," *Biotechnology and bioengineering*, vol. 78, no. 4, pp. 467–472, 2002, doi: 10.1002/bit.10212.

[4]   Y. Kostov, P. Harms, L. Randers-Eichhorn, and G. Rao, "Low-cost microbioreactor for high-throughput bioprocessing," *Biotechnol. Bioeng.*, vol. 72, no. 3, pp. 346–352, 2001, doi: 10.1002/1097-0290(20010205)72:3<346::AID-BIT12>3.0.CO;2-X.

[5]   J. F. Gouin, F. Baros, D. Birot, and J. C. André, "A fibre-optic oxygen sensor for oceanography," *Sensors and Actuators B: Chemical*, vol. 39, 1-3, pp. 401–406, 1997, doi: 10.1016/S0925-4005(97)80242-0.

[6]   C. R. Schröder, B. M. Weidgans, and I. Klimant, "pH fluorosensors for use in marine systems," *The Analyst*, vol. 130, no. 6, pp. 907–916, 2005, doi: 10.1039/B501306B.

[7]   A. Fernandes-Platzgummer, M. M. Diogo, C. Lobato da Silva, and J. M.S. Cabral, "Maximizing mouse embryonic stem cell production in a stirred tank reactor by controlling dissolved oxygen concentration and continuous perfusion operation," *Biochemical Engineering Journal*, vol. 82, pp. 81–90, 2014, doi: 10.1016/j.bej.2013.11.014.

[8]   P. O'Mara, A. Farrell, J. Bones, and K. Twomey, "Staying alive! Sensors used for monitoring cell health in bioreactors," *Talanta*, vol. 176, pp. 130–139, 2018, doi: 10.1016/j.talanta.2017.07.088.

[9]   I. M. McLeod *et al.,* "Climate change and the performance of larval coral reef fishes: the interaction between temperature and food availability," *Conservation physiology*, vol. 1, no. 1, cot024, 2013, doi: 10.1093/conphys/cot024.

[10] L. Chipman *et al.,* "Oxygen optodes as fast sensors for eddy correlation measurements in aquatic systems," *Limnol. Oceanogr. Methods*, vol. 10, no. 5, pp. 304–316, 2012, doi: 10.4319/lom.2012.10.304.

[11] P. Berg and M. Huettel, "Monitoring the Seafloor Using the Noninvasive Eddy Correlation Technique: Integrated Benthic Exchange Dynamics," *Oceanography*, vol. 21, no. 4, pp. 164–167, 2008. [Online]. Available: www.jstor.org/stable/24860020

[12] L. C. CLARK, R. WOLF, D. GRANGER, and Z. TAYLOR, "Continuous recording of blood oxygen tensions by polarography," *Journal of applied physiology*, vol. 6, no. 3, pp. 189–193, 1953, doi: 10.1152/jappl.1953.6.3.189.

[13] P. T. Kerridge, "The Use of the Glass Electrode in Biochemistry," *The Biochemical journal*, vol. 19, no. 4, pp. 611–617, 1925, doi: 10.1042/bj0190611.

[14] C. McDonagh, C. S. Burke, and B. D. MacCraith, "Optical chemical sensors," *Chemical reviews*, vol. 108, no. 2, pp. 400–422, 2008, doi: 10.1021/cr068102g.

[15] X.-d. Wang and O. S. Wolfbeis, "Optical methods for sensing and imaging oxygen: materials, spectroscopies and applications," *Chemical Society reviews*, vol. 43, no. 10, pp. 3666–3761, 2014, doi: 10.1039/C4CS00039K.

[16] M. Quaranta, S. M. Borisov, and I. Klimant, "Indicators for optical oxygen sensors," *Bioanalytical reviews*, vol. 4, 2-4, pp. 115–157, 2012, doi: 10.1007/s12566-012-0032-y.

[17] Y. Amao, "Probes and Polymers for Optical Sensing of Oxygen," *Microchimica Acta*, vol. 143, no. 1, pp. 1–12, 2003, doi: 10.1007/s00604-003-0037-x.

[18] M. I. Khan, K. Mukherjee, R. Shoukat, and H. Dong, "A review on pH sensitive materials for sensors and detection methods," *Microsyst Technol*, vol. 23, no. 10, pp. 4391–4404, 2017, doi: 10.1007/s00542-017-3495-5.

[19] D. Wencel, T. Abel, and C. McDonagh, "Optical chemical pH sensors," *Analytical chemistry*, vol. 86, no. 1, pp. 15–29, 2014, doi: 10.1021/ac4035168.

[20] S. M. Grist, L. Chrostowski, and K. C. Cheung, "Optical oxygen sensors for applications in microfluidic cell culture," *Sensors (Basel, Switzerland)*, vol. 10, no. 10, pp. 9286–9316, 2010, doi: 10.3390/s101009286.

[21] A. Richter, G. Paschew, S. Klatt, J. Lienig, K.-F. Arndt, and H.-J. P. Adler, "Review on Hydrogel-based pH Sensors and Microsensors," *Sensors (Basel, Switzerland)*, vol. 8, no. 1, pp. 561–581, 2008, doi: 10.3390/s8010561.

[22] J. Han and K. Burgess, "Fluorescent indicators for intracellular pH," *Chemical reviews*, vol. 110, no. 5, pp. 2709–2728, 2010, doi: 10.1021/cr900249z.

[23] J. R. Lakowicz and G. Weber, "Quenching of fluorescence by oxygen. A probe for structural fluctuations in macromolecules," *Biochemistry*, vol. 12, no. 21, pp. 4161–4170, 1973, doi: 10.1021/bi00745a020.

[24] H.-C. Hesse, "Meßsonde," DD106086A1, German Democratic Republic.

[25] J. I. Peterson, R. V. Fitzgerald, and D. K. Buckhold, "Fiber-optic probe for in vivo measurement of oxygen partial pressure," *Analytical chemistry*, vol. 56, no. 1, pp. 62–67, 1984, doi: 10.1021/ac00265a017.

[26] M. E. Lippitsch, J. Pusterhofer, M. J.P. Leiner, and O. S. Wolfbeis, "Fibre-optic oxygen sensor with the fluorescence decay time as the information carrier," *Analytica Chimica Acta*, vol. 205, pp. 1–6, 1988, doi: 10.1016/S0003-2670(00)82310-7.

[27] O. S. Wolfbeis, M. J. P. Leiner, and H. E. Posch, "A new sensing material for optical oxygen measurement, with the indicator embedded in an aqueous phase," *Mikrochim Acta*, vol. 90, 5-6, pp. 359–366, 1986, doi: 10.1007/BF01199278.

[28] S.-K. Lee and I. Okura, "Photostable Optical Oxygen Sensing Material: Platinum Tetrakis(pentafluorophenyl)porphyrin Immobilized in Polystyrene," *Anal. Commun.*, vol. 34, no. 6, pp. 185–188, 1997, doi: 10.1039/A701130J.

[29] S.-K. Lee and I. Okura, "Optical Sensor for Oxygen Using a Porphyrin-doped Sol–Gel Glass," *Analyst*, vol. 122, no. 1, pp. 81–84, 1997, doi: 10.1039/A604885D.

[30] D. B. Papkovsky, G. V. Ponomarev, W. Trettnak, and P. O'Leary, "Phosphorescent Complexes of Porphyrin Ketones: Optical Properties and Application to Oxygen Sensing," *Anal. Chem.*, vol. 67, no. 22, pp. 4112–4117, 1995, doi: 10.1021/ac00118a013.

[31] I. Klimant, V. Meyer, and M. Kühl, "Fiber-optic oxygen microsensors, a new tool in aquatic biology," *Limnol. Oceanogr.*, vol. 40, no. 6, pp. 1159–1165, 1995, doi: 10.4319/lo.1995.40.6.1159.

[32] I. Klimant, M. Kühl, R. N. Glud, and G. Holst, "Optical measurement of oxygen and temperature in microscale: Strategies and biological applications," *Sensors and Actuators B: Chemical*, vol. 38, 1-3, pp. 29–37, 1997, doi: 10.1016/S0925-4005(97)80168-2.

[33] H. Schmidt-Böcking, K. Reich, A. Templeton, W. Trageser, and V. Vill, *Otto Sterns Veröffentlichungen – Band 2*. Berlin, Heidelberg: Springer Berlin Heidelberg, 2016.

[34] W. der Wissenschaft, "Max Volmer (1885–1965)," in *"The shoulders on which we stand"-Wegbereiter der Wissenschaft*, E. Knobloch, Ed., Berlin, Heidelberg: Springer Berlin Heidelberg, 2004, pp. 194–197.

[35] P. S. Chelushkin and S. P. Tunik, "Phosphorescence Lifetime Imaging (PLIM): State of the Art and Perspectives," in *Springer Series in Chemical Physics, Progress in Photon Science*, K. Yamanouchi, S. Tunik, and V. Makarov, Eds., Cham: Springer International Publishing, 2019, pp. 109–128.

[36] L. S. Foster and I. J. Gruntfest, "Demonstration experiments using universal indicators," *J. Chem. Educ.*, vol. 14, no. 6, p. 274, 1937, doi: 10.1021/ed014p274.

[37] H. Wenker, "Indicator Paper," United States of America 2,229,155.

[38] J. I. Peterson, S. R. Goldstein, R. V. Fitzgerald, and D. K. Buckhold, "Fiber optic pH probe for physiological use," *Anal. Chem.*, vol. 52, no. 6, pp. 864–869, 1980, doi: 10.1021/ac50056a022.

[39] L. A. Saari and W. R. Seitz, "pH sensor based on immobilized fluoresceinamine," *Anal. Chem.*, vol. 54, no. 4, pp. 821–823, 1982, doi: 10.1021/ac00241a052.

[40] Z. Zhujun and W.R. Seitz, "A fluorescence sensor for quantifying pH in the range from 6.5 to 8.5," *Analytica Chimica Acta*, vol. 160, pp. 47–55, 1984, doi: 10.1016/S0003-2670(00)84507-9.

[41] K. T.v. Grattan, Z. Mouaziz, and R. K. Selli, "Ph Sensor Using A LED Source In A Fibre Optic Device," in *Fiber Optic Sensors II*, 1987, pp. 230–237.

[42] E. T. Knobbe, B. Dunn, and M. Gold, "Organic Molecules Entrapped In A Silica Host For Use As Biosensor Probe Materials," in *Optical Fibers in Medicine III*, Los Angeles, CA, 1988, p. 39.

[43] G. E. Badini, K. T. V. Grattan, and A. C. C. Tseung, "Sol‐gels with fiber‐optic chemical sensor potential: Effects of preparation, aging, and long‐term storage," *Review of Scientific Instruments*, vol. 66, no. 8, pp. 4034–4040, 1995, doi: 10.1063/1.1145413.

[44] G. E. Badini, K.T.V. Grattan, A.C.C. Tseung, and A. W. Palmer, "Sol-Gel Properties for Fiber Optic Sensor Applications," *Optical Fiber Technology*, vol. 2, no. 4, pp. 378–386, 1996, doi: 10.1006/ofte.1996.0043.

[45] G. E. Badini, K. T. V. Grattan, and A. C. C. Tseung, "Impregnation of a pH-sensitive dye into sol–gels for fibre optic chemical sensors," *Analyst*, vol. 120, no. 4, pp. 1025–1028, 1995, doi: 10.1039/AN9952001025.

[46] A. Song, S. Parus, and R. Kopelman, "High-performance fiber-optic pH microsensors for practical physiological measurements using a dual-emission sensitive dye," *Anal. Chem.*, vol. 69, no. 5, pp. 863–867, 1997, doi: 10.1021/ac960917+.

[47] M. E. Lippitsch, S. Draxler, and M. J. P. Leiner, "Time-domain fluorescence methods as applied to pH sensing," in *Chemical, Biochemical, and Environmental Fiber Sensors IV*, Boston, MA, 1993, pp. 202–209.

[48] I. Klimant, C. Huber, G. Liebsch, G. Neurauter, A. Stangelmayer, and O. S. Wolfbeis, "Dual Lifetime Referencing (DLR) — a New Scheme for Converting Fluorescence Intensity into a Frequency-Domain or Time-Domain Information," in *Springer Series on Fluorescence, New Trends in Fluorescence Spectroscopy*, O. Wolfbeis, B. Valeur, and J.-C. Brochon, Eds., Berlin, Heidelberg: Springer Berlin Heidelberg, 2001, pp. 257–274.

[49] G. A. Tait, R. B. Young, G. J. Wilson, D. J. Steward, and D. C. MacGregor, "Myocardial pH during regional ischemia: evaluation of a fiber-optic photometric probe," *The American journal of physiology*, vol. 243, no. 6, H1027-31, 1982, doi: 10.1152/ajpheart.1982.243.6.H1027.

[50] J. R. Lakowicz, Ed., *Principles of Fluorescence Spectroscopy*. Boston, MA: Springer US, 2006.

[51] G. G. Stokes, "On the change of refrangibility of light," *Phil. Trans. R. Soc.*, vol. 142, pp. 463–562, 1852, doi: 10.1098/rstl.1852.0022.

[52] N. Ioannides *et al.,* "Approaches to mitigate polymer-core loss in plastic optical fibers: a review," *Mater. Res. Express*, vol. 1, no. 3, p. 32002, 2014, doi: 10.1088/2053-1591/1/3/032002.

[53] S. Medina-Rodríguez, Á. de La Torre-Vega, C. Medina-Rodríguez, J. F. Fernández-Sánchez, and A. Fernández-Gutiérrez, "On the calibration of chemical sensors based on photoluminescence: Selecting the appropriate optimization criterion," *Sensors and Actuators B: Chemical*, vol. 212, pp. 278–286, 2015, doi: 10.1016/j.snb.2015.02.022.

[54] T. Förster, "Zwischenmolekulare Energiewanderung und Fluoreszenz," *Ann. Phys.*, vol. 437, 1-2, pp. 55–75, 1948, doi: 10.1002/andp.19484370105.

[55] G. A. Jones and D. S. Bradshaw, "Resonance Energy Transfer: From Fundamental Theory to Recent Applications," *Front. Phys.*, vol. 7, 2019, doi: 10.3389/fphy.2019.00100.

[56] S. P. L. Sørensen, "Enzymstudien II: Über die Messung und die Bedeutung der Wasserstoffionenkonzentration bei enzymatischen Prozessen," in *Biochem. Zeit.*, pp. 131–304.

[57] A. S. Vasylevska, A. A. Karasyov, S. M. Borisov, and C. Krause, "Novel coumarin-based fluorescent pH indicators, probes and membranes covering a broad pH range," *Analytical and bioanalytical chemistry*, vol. 387, no. 6, pp. 2131–2141, 2007, doi: 10.1007/s00216-006-1061-6.

[58] I. Klimant and O. S. Wolfbeis, "Oxygen-Sensitive Luminescent Materials Based on Silicone-Soluble Ruthenium Diimine Complexes," *Anal. Chem.*, vol. 67, no. 18, pp. 3160–3166, 1995, doi: 10.1021/ac00114a010.

[59] F. Mohamad *et al.,* "Controlled core-to-core photo-polymerisation - fabrication of an optical fibre-based pH sensor," *The Analyst*, vol. 142, no. 19, pp. 3569–3572, 2017, doi: 10.1039/c7an00454k.

[60] T. H. Nguyen, T. Venugopalan, T. Sun, and K. T. V. Grattan, "Intrinsic Fiber Optic pH Sensor for Measurement of pH Values in the Range of 0.5–6," *IEEE Sensors J.*, vol. 16, no. 4, pp. 881–887, 2016, doi: 10.1109/JSEN.2015.2490583.

[61] G. A. Holst, M. Kuehl, and I. Klimant, "<title>Novel measuring system for oxygen micro-optodes based on a phase modulation technique</title>," in *European Symposium on Optics for Environmental and Public Safety*, Munich, Germany, 1995, pp. 387–398.

[62] C.-S. Chu and Y.-L. Lo, "Highly sensitive and linear calibration optical fiber oxygen sensor based on Pt(II) complex embedded in sol–gel matrix," *Sensors and Actuators B: Chemical*, vol. 155, no. 1, pp. 53–57, 2011, doi: 10.1016/j.snb.2010.11.023.

[63] C.-S. Chu and Y.-L. Lo, "High-performance fiber-optic oxygen sensors based on fluorinated xerogels doped with Pt(II) complexes," *Sensors and Actuators B: Chemical*, vol. 124, no. 2, pp. 376–382, 2007, doi: 10.1016/j.snb.2006.12.049.

[64] G. R. McDowell, A. S. Holmes-Smith, M. Uttamlal, C. Mitchell, and P. H. Shannon, "A robust and reliable optical trace oxygen sensor," *SPIE, Optical Sensors*, Vol. 10231, 2017, doi: 10.1117/12.2265561.

[65] L. Ferrari, L. Rovati, P. Fabbri, and F. Pilati, "Disposable fluorescence optical pH sensor for near neutral solutions," *Sensors (Basel, Switzerland)*, vol. 13, no. 1, pp. 484–499, 2012, doi: 10.3390/s130100484.

[66] Y. Xiong *et al.,* "A miniaturized oxygen sensor integrated on fiber surface based on evanescent-wave induced fluorescence quenching," *Journal of Luminescence*, vol. 179, pp. 581–587, 2016, doi: 10.1016/j.jlumin.2016.08.005.

[67] S. A. Mousavi Shaegh *et al.,* "A microfluidic optical platform for real-time monitoring of pH and oxygen in microfluidic bioreactors and organ-on-chip devices," *Biomicrofluidics*, vol. 10, no. 4, p. 44111, 2016, doi: 10.1063/1.4955155.

[68] U. Kosch, I. Klimant, and O. S. Wolfbeis, "Long-lifetime based pH micro-optodes without oxygen interference," *Fresenius' Journal of Analytical Chemistry*, vol. 364, 1-2, pp. 48–53, 1999, doi: 10.1007/s002160051299.

[69] C. McDonagh *et al.,* "Phase fluorometric dissolved oxygen sensor," *Sensors and Actuators B: Chemical*, vol. 74, 1-3, pp. 124–130, 2001, doi: 10.1016/S0925-4005(00)00721-8.

[70] G. O'Keeffe, B. D. MacCraith, A. K. McEvoy, C. M. McDonagh, and J. F. McGilp, "Development of a LED-based phase fluorimetric oxygen sensor using evanescent wave excitation of a sol-gel immobilized dye," *Sensors and Actuators B: Chemical*, vol. 29, 1-3, pp. 226–230, 1995, doi: 10.1016/0925-4005(95)01687-2.

[71] C.-S. Chu, K.-Z. Lin, and Y.-H. Tang, "A new optical sensor for sensing oxygen based on phase shift detection," *Sensors and Actuators B: Chemical*, vol. 223, pp. 606–612, 2016, doi: 10.1016/j.snb.2015.09.155.

[72] V. I. Ogurtsov and D. B. Papkovsky, "Selection of modulation frequency of excitation for luminescence lifetime-based oxygen sensors," *Sensors and Actuators B: Chemical*, vol. 51, 1-3, pp. 377–381, 1998, doi: 10.1016/S0925-4005(98)00209-3.

[73] M. E. Lippitsch and S. Draxler, "Luminescence decay-time-based optical sensors: principles and problems," *Sensors and Actuators B: Chemical*, vol. 11, 1-3, pp. 97–101, 1993, doi: 10.1016/0925-4005(93)85243-4.

[74] S. Medina-Rodríguez, C. Medina-Rodríguez, Á. de La Torre-Vega, J. C. Segura-Luna, S. Mota-Fernández, and J. F. Fernández-Sánchez, "Real-time optimal combination of multifrequency information in phase-resolved luminescence spectroscopy based on rectangular-wave signals," *Sensors and Actuators B: Chemical*, vol. 238, pp. 221–225, 2017, doi: 10.1016/j.snb.2016.07.046.

[75] S. Medina-Rodríguez *et al.,* "Improved multifrequency phase-modulation method that uses rectangular-wave signals to increase accuracy in luminescence spectroscopy," *Analytical chemistry*, vol. 86, no. 11, pp. 5245–5256, 2014, doi: 10.1021/ac4030895.

[76] S. Medina-Rodríguez, A. de La Torre-Vega, J. F. Fernández-Sánchez, and A. Fernández-Gutiérrez, "An open and low-cost optical-fiber measurement system for the optical detection of oxygen using a multifrequency phase-resolved method," *Sensors and Actuators B: Chemical*, vol. 176, pp. 1110–1120, 2013, doi: 10.1016/j.snb.2012.09.051.

[77] E. Schmälzlin *et al.,* "An optical multifrequency phase-modulation method using microbeads for measuring intracellular oxygen concentrations in plants," *Biophysical journal*, vol. 89, no. 2, pp. 1339–1345, 2005, doi: 10.1529/biophysj.105.063453.

[78] B. Valeur and M. N. Berberan-Santos, *Molecular Fluorescence: Principles and applications,* 2nd ed. Weinheim: Wiley-VCH, 2013. [Online]. Available: https://onlinelibrary.wiley.com/doi/book/10.1002/9783527650002

[79] R. M. Ballew and J. N. Demas, "An error analysis of the rapid lifetime determination method for the evaluation of single exponential decays," *Anal. Chem.*, vol. 61, no. 1, pp. 30–33, 1989, doi: 10.1021/ac00176a007.

[80] I. Klimant, F. Ruckruh, G. Liebsch, A. Stangelmayer, and O. S. Wolfbeis, "Fast Response Oxygen Micro-Optodes Based on Novel Soluble Ormosil Glasses," *Microchimica Acta*, vol. 131, 1-2, pp. 35–46, 1999, doi: 10.1007/s006040050007.

[81] G. Holst, R. N. Glud, M. Kühl, and I. Klimant, "A microoptode array for fine-scale measurement of oxygen distribution," *Sensors and Actuators B: Chemical*, vol. 38, 1-3, pp. 122–129, 1997, doi: 10.1016/S0925-4005(97)80181-5.

[82] G. H. Ingo Klimant, "OPTICAL TEMPERATURE SENSORS AND OPTICAL-CHEMICAL SENSORS WITH OPTICAL TEMPERATURE COMPENSATION," US 6,303,386 B2, Germany, Oct 16, 2001.

[83] F. Wang *et al.,* "Optical fiber oxygen sensor utilizing a robust phase demodulator," *Measurement*, vol. 95, pp. 1–7, 2017, doi: 10.1016/j.measurement.2016.09.022.

[84] C. Jia, J. Chang, F. Wang, H. Jiang, C. Zhu, and P. Wang, "A Phase Shift Demodulation Technique: Verification and Application in Fluorescence Phase Based Oxygen Sensors," *Photonic Sens*, vol. 6, no. 2, pp. 169–176, 2016, doi: 10.1007/s13320-016-0303-2.

[85] M. I. J. Stich, L. H. Fischer, and O. S. Wolfbeis, "Multiple fluorescent chemical sensing and imaging," *Chemical Society reviews*, vol. 39, no. 8, pp. 3102–3114, 2010, doi: 10.1039/b909635n.

[86] B. H. Weigl *et al.,* "Optical triple sensor for measuring pH, oxygen and carbon dioxide," *Journal of Biotechnology*, vol. 32, no. 2, pp. 127–138, 1994, doi: 10.1016/0168-1656(94)90175-9.

[87] C.-S. Chu and T.-H. Lin, "A new portable optical sensor for dual sensing of temperature and oxygen," *Sensors and Actuators B: Chemical*, vol. 202, pp. 508–515, 2014, doi: 10.1016/j.snb.2014.05.125.

[88] M. I. J. Stich, S. Nagl, O. S. Wolfbeis, U. Henne, and M. Schaeferling, "A Dual Luminescent Sensor Material for Simultaneous Imaging of Pressure and Temperature on Surfaces," *Adv. Funct. Mater.*, vol. 18, no. 9, pp. 1399–1406, 2008, doi: 10.1002/adfm.200701199.

[89] C. R. Schröder, L. Polerecky, and I. Klimant, "Time-resolved pH/pO2 mapping with luminescent hybrid sensors," *Anal. Chem.*, vol. 79, no. 1, pp. 60–70, 2007, doi: 10.1021/ac0606047.

[90] C.-S. Chu and C.-A. Lin, "Optical fiber sensor for dual sensing of temperature and oxygen based on PtTFPP/CF embedded in sol–gel matrix," *Sensors and Actuators B: Chemical*, vol. 195, pp. 259–265, 2014, doi: 10.1016/j.snb.2014.01.032.

[91] G. Liebsch, I. Klimant, C. Krause, and O. S. Wolfbeis, "Fluorescent imaging of pH with optical sensors using time domain dual lifetime referencing," *Analytical chemistry*, vol. 73, no. 17, pp. 4354–4363, 2001, doi: 10.1021/ac0100852.

[92] S. M. Borisov and O. S. Wolfbeis, "Temperature-sensitive europium(III) probes and their use for simultaneous luminescent sensing of temperature and oxygen," *Anal. Chem.*, vol. 78, no. 14, pp. 5094–5101, 2006, doi: 10.1021/ac060311d.

[93] J. Hradil, C. Davis, K. Mongey, C. McDonagh, and B. D. MacCraith, "Temperature-corrected pressure-sensitive paint measurements using a single camera and a dual-lifetime approach," *Meas. Sci. Technol.*, vol. 13, no. 10, pp. 1552–1557, 2002, doi: 10.1088/0957-0233/13/10/307.

[94]   A. Steinegger, O. S. Wolfbeis, and S. M. Borisov, "Optical Sensing and Imaging of pH Values: Spectroscopies, Materials, and Applications," *Chemical reviews*, vol. 120, no. 22, pp. 12357–12489, 2020, doi: 10.1021/acs.chemrev.0c00451.

[95]   C. Wolf, M. Tscherner, and S. Köstler, "Ultra-fast opto-chemical sensors by using electrospun nanofibers as sensing layers," *Sensors and Actuators B: Chemical*, vol. 209, pp. 1064–1069, 2015, doi: 10.1016/j.snb.2014.11.070.

[96]   M. Rosenberg, B. W. Laursen, C. G. Frankær, and T. J. Sørensen, "A Fluorescence Intensity Ratiometric Fiber Optics–Based Chemical Sensor for Monitoring pH," *Adv. Mater. Technol.*, vol. 3, no. 12, p. 1800205, 2018, doi: 10.1002/admt.201800205.

[97]   P. Gruber, M. P. C. Marques, N. Szita, and T. Mayr, "Integration and application of optical chemical sensors in microbioreactors," *Lab on a chip*, vol. 17, no. 16, pp. 2693–2712, 2017, doi: 10.1039/c7lc00538e.

[98]   B. Ungerböck, V. Charwat, P. Ertl, and T. Mayr, "Microfluidic oxygen imaging using integrated optical sensor layers and a color camera," *Lab on a chip*, vol. 13, no. 8, pp. 1593–1601, 2013, doi: 10.1039/c3lc41315b.

[99]   M. ajlakovi et al., "Optochemical Sensor Systems for In-Vivo Continuous Monitoring of Blood Gases in Adipose Tissue and in Vital Organs," in *Advances in Chemical Sensors*, W. Wang, Ed.: InTech, 2012.

[100]   J. P. Fischer and K. Koop-Jakobsen, "The multi fiber optode (MuFO): A novel system for simultaneous analysis of multiple fiber optic oxygen sensors," *Sensors and Actuators B: Chemical*, vol. 168, pp. 354–359, 2012, doi: 10.1016/j.snb.2012.04.034.

[101]   E. Trampe et al., "Functionalized Bioink with Optical Sensor Nanoparticles for O 2 Imaging in 3D-Bioprinted Constructs," *Adv. Funct. Mater.*, vol. 28, no. 45, p. 1804411, 2018, doi: 10.1002/adfm.201804411.

[102]   S. Addanki, I. S. Amiri, and P. Yupapin, "Review of optical fibers-introduction and applications in fiber lasers," *Results in Physics*, vol. 10, pp. 743–750, 2018, doi: 10.1016/j.rinp.2018.07.028.

[103]   G. S. Glaesemann, "Advancements in mechanical strength and reliability of optical fibers," in *Reliability of Optical Fibers and Optical Fiber Systems: A Critical Review*, Bellingham, United States, 2017, p. 1029502.

[104]   C. Sonnenfeld et al., "Mechanical Strength of Microstructured Optical Fibers," *J. Lightwave Technol.*, vol. 32, no. 12, pp. 2193–2201, 2014.

[105]   A. Méndez and T. F. Morse, Eds., *Specialty optical fibers handbook*. Amsterdam, Birmingham, AL, USA: Academic Press; EBSCO Industries Inc, 2007.

[106]   O. Ziemann, J. Krauser, P. E. Zamzow, and W. Daum, *POF Handbook: Optical Short Range Transmission Systems,* 2nd ed. Berlin, Heidelberg, Cham: Springer Berlin Heidelberg; Springer International Publishing AG, 2008.

[107]   J. Heimann, P. Raithel, T. Tobisch, M. Belz, and K.-F. Klein, "Light-guidance in step-index fibers with non-circular shaped core," in *Micro-structured and Specialty Optical Fibres IV*, Prague, Czech Republic, 2015, 95070R.

[108]   K. Kalli and A. Mendez, Eds., *Micro-Structured and Specialty Optical Fibres IV*: SPIE, 2016.

[109]   H. Ohlmeyer, T. Tobisch, M. M. A. J. Voncken, L. Prechtel, M. Belz, and K.-F. Klein, "Influence of fiber design on light-guidance in step-index fibers for bundle applications in the UV-VIS-region," in *Micro-structured and Specialty Optical Fibres III*, Brussels, Belgium, 2014, p. 912809.

[110] S. Ferwana *et al.,* "All-silica fiber with low or medium OH-content for broadband applications in astronomy," in *Optical Fabrication, Metrology, and Material Advancements for Telescopes*, USA, 2004, p. 598.

[111] E. Arrospide, I. Bikandi, I. García, G. Durana, G. Aldabaldetreku, and J. Zubia, "Mechanical properties of polymer-optical fibres," in *Polymer Optical Fibres*: Elsevier, 2017, pp. 201–216.

[112] J. Zubia and J. Arrue, "Plastic Optical Fibers: An Introduction to Their Technological Processes and Applications," *Optical Fiber Technology*, vol. 7, no. 2, pp. 101–140, 2001, doi: 10.1006/ofte.2000.0355.

[113] D.F. Merchant, P.J. Scully, and N.F. Schmitt, "Chemical tapering of polymer optical fibre," *Sensors and Actuators A: Physical*, vol. 76, 1-3, pp. 365–371, 1999, doi: 10.1016/S0924-4247(99)00008-4.

[114] A. K. Pathak, V. Bhardwaj, R. K. Gangwar, M. De, and V. K. Singh, "Fabrication and characterization of TiO 2 coated cone shaped nano-fiber pH sensor," *Optics Communications*, vol. 386, pp. 43–48, 2017, doi: 10.1016/j.optcom.2016.11.021.

[115] B. Grunwald and G. Holst, "Fibre optic refractive index microsensor based on white-light SPR excitation," *Sensors and Actuators A: Physical*, vol. 113, no. 2, pp. 174–180, 2004, doi: 10.1016/j.sna.2004.02.014.

[116] J. Werner, M. Belz, K.-F. Klein, T. Sun, and K.T.V. Grattan, "Fast response time fiber optical pH and oxygen sensors," in *Optical Fibers and Sensors for Medical Diagnostics and Treatment Applications XX*, San Francisco, United States, Feb. 2020 - Feb. 2020, p. 56. [Online]. Available: https://www.spiedigitallibrary.org/conference-proceedings-of-spie/11233/2566993/Fast-response-time-fiber-optical-pH-and-oxygen-sensors/10.1117/12.2566993.full

[117] L. F. Rickelt, L. D.M. Ottosen, and M. Kühl, "Etching of multimode optical glass fibers: A new method for shaping the measuring tip and immobilization of indicator dyes in recessed fiber-optic microprobes," *Sensors and Actuators B: Chemical*, vol. 211, pp. 462–468, 2015, doi: 10.1016/j.snb.2015.01.091.

[118] M. Zolkapli, S. Saharudin, S. H. Herman, and W. F. H. Abdullah, "Quasi-distributed sol-gel coated fiber optic oxygen sensing probe," *Optical Fiber Technology*, vol. 41, pp. 109–117, 2018, doi: 10.1016/j.yofte.2017.12.016.

[119] S. Singh and B. D. Gupta, "Fabrication and characterization of a highly sensitive surface plasmon resonance based fiber optic pH sensor utilizing high index layer and smart hydrogel," *Sensors and Actuators B: Chemical*, vol. 173, pp. 268–273, 2012, doi: 10.1016/j.snb.2012.06.089.

[120] N. K. Sharma and B. D. Gupta, "Fabrication and characterization of pH sensor based on side polished single mode optical fiber," *Optics Communications*, vol. 216, 4-6, pp. 299–303, 2003, doi: 10.1016/S0030-4018(02)02343-X.

[121] M. R. R. Khan and S.-W. Kang, "Highly Sensitive and Wide-Dynamic-Range Multichannel Optical-Fiber pH Sensor Based on PWM Technique," *Sensors (Basel, Switzerland)*, vol. 16, no. 11, 2016, doi: 10.3390/s16111885.

[122] B. D. Gupta and N. K. Sharma, "Fabrication and characterization of U-shaped fiber-optic pH probes," *Sensors and Actuators B: Chemical*, vol. 82, no. 1, pp. 89–93, 2002, doi: 10.1016/S0925-4005(01)00995-9.

[123] F. Surre *et al.,* "U-bend fibre optic pH sensors using layer-by-layer electrostatic self-assembly technique," *J. Phys.: Conf. Ser.*, vol. 178, p. 12046, 2009, doi: 10.1088/1742-6596/178/1/012046.

[124] J. Zajíc, L. Traplová, V. Matějec, M. Pospíšilová, and I. Bartoň, "Optical pH Detection with U-Shaped Fiber-Optic Probes and Absorption Transducers," *Conference Papers in Science*, vol. 2015, pp. 1–8, 2015, doi: 10.1155/2015/513621.

[125] S. Chen, Q. Yang, H. Xiao, H. Shi, and Y. Ma, "Local pH Monitoring of Small Cluster of Cells using a Fiber-Optic Dual-Core Micro-Probe," *Sensors and Actuators B: Chemical*, vol. 241, pp. 398–405, 2017, doi: 10.1016/j.snb.2016.10.079.

[126] Q. Yang *et al.,* "Fiber-Optic-Based Micro-Probe Using Hexagonal 1-in-6 Fiber Configuration for Intracellular Single-Cell pH Measurement," *Analytical chemistry*, vol. 87, no. 14, pp. 7171–7179, 2015, doi: 10.1021/acs.analchem.5b01040.

[127] T. H. Nguyen *et al.,* "Fluorescence based fibre optic pH sensor for the pH 10–13 range suitable for corrosion monitoring in concrete structures," *Sensors and Actuators B: Chemical*, vol. 191, pp. 498–507, 2014, doi: 10.1016/j.snb.2013.09.072.

[128] C. G. Frankær, K. J. Hussain, T. C. Dörge, and T. J. Sørensen, "Optical Chemical Sensor Using Intensity Ratiometric Fluorescence Signals for Fast and Reliable pH Determination," *ACS sensors*, vol. 4, no. 1, pp. 26–31, 2019, doi: 10.1021/acssensors.8b01485.

[129] C. Staudinger *et al.,* "A versatile optode system for oxygen, carbon dioxide, and pH measurements in seawater with integrated battery and logger," *Limnol. Oceanogr. Methods*, vol. 16, no. 7, pp. 459–473, 2018, doi: 10.1002/lom3.10260.

[130] PyroScience GmbH, *PHROBSC-PK6: Robust pH Screw Cap Probe*. Datasheet. [Online]. Available: https://www.pyroscience.com/en/products/all-sensors/phrobsc-pk6#Downloads (accessed: Nov. 24 2020).

[131] PreSens Precision Sensing GmbH, *PM-PSt1: Oxygen Microsensor.* [Online]. Available: https://www.presens.de/products/detail/profiling-oxygen-microsensor-pm-pst1 (accessed: Nov. 24 2020).

[132] C.-S. Chu and C.-Y. Chuang, "Highly sensitive fiber-optic oxygen sensor based on palladium tetrakis (4-carboxyphenyl)porphyrin doped in ormosil," *Journal of Luminescence*, vol. 154, pp. 475–478, 2014, doi: 10.1016/j.jlumin.2014.05.025.

[133] Ingo Klimant, Hellfried Karpf, Otto S. Wolfbeis, "Sensor membrane of an optical sensor," US6139798A, Switzerland, Oct 31, 2000.

[134] "Optical sensor for measuring an analyte and method of manufacturing the same," EP1199556A1, Switzerland, Nov 25, 2003.

[135] Ingo Klimant, "Method and device for referencing fluorescence intensity signals," US6602716B1, Germany, Aug 5, 2003.

[136] Ingo Klimant, "Sensor for luminescense-optical determination of an analyte," US7067320B2, Jul 11, 2002.

[137] PreSens Precision Sensing GmbH, *FTCH-PSt1: Flow-Through Cell Housed Oxygen Microsensor.* [Online]. Available: https://www.presens.de/products/detail/flow-through-cell-housed-oxygen-microsensor-ftch-pst1 (accessed: Nov. 24 2020).

[138] Mahmoud R. Shahriari, "Method and composition for a platinum embedded sol gel optical chemical sensor with improved sensitivity and chemical stability," US20080199360A1, Aug 21, 2008.

[139] Ocean Insight, Inc., *Oxygen Sensor Probes.* [Online]. Available: https://www.oceaninsight.com/products/sampling-accessories/sensors/oxygen/oxygen-probes/ (accessed: Nov. 24 2020).

[140] T. Jokic, S. M. Borisov, R. Saf, D. A. Nielsen, M. Kühl, and I. Klimant, "Highly photostable near-infrared fluorescent pH indicators and sensors based on BF2-chelated tetraarylazadipyrromethene dyes," *Analytical chemistry*, vol. 84, no. 15, pp. 6723–6730, 2012, doi: 10.1021/ac3011796.

[141] M. Strobl, T. Rappitsch, S. M. Borisov, T. Mayr, and I. Klimant, "NIR-emitting aza-BODIPY dyes--new building blocks for broad-range optical pH sensors," *Analyst*, vol. 140, no. 21, pp. 7150–7153, 2015, doi: 10.1039/C5AN01389E.

[142] F. Niedermair *et al.,* "Tunable phosphorescent NIR oxygen indicators based on mixed benzo- and naphthoporphyrin complexes," *Inorganic chemistry*, vol. 49, no. 20, pp. 9333–9342, 2010, doi: 10.1021/ic100955z.

[143] S. M. Borisov, G. Nuss, and I. Klimant, "Red light-excitable oxygen sensing materials based on platinum(II) and palladium(II) benzoporphyrins," *Analytical chemistry*, vol. 80, no. 24, pp. 9435–9442, 2008, doi: 10.1021/ac801521v.

[144] Y.-E. K. Lee *et al.,* "Near infrared luminescent oxygen nanosensors with nanoparticle matrix tailored sensitivity," *Analytical chemistry*, vol. 82, no. 20, pp. 8446–8455, 2010, doi: 10.1021/ac1015358.

[145] S. M. Borisov, K. Gatterer, B. Bitschnau, and I. Klimant, "Preparation and Characterization of Chromium(III)-Activated Yttrium Aluminum Borate: A New Thermographic Phosphor for Optical Sensing and Imaging at Ambient Temperatures," *The journal of physical chemistry. C, Nanomaterials and interfaces*, vol. 114, no. 19, pp. 9118–9124, 2010, doi: 10.1021/jp1016467.

[146] E. Fritzsche *et al.,* "Highly sensitive poisoning-resistant optical carbon dioxide sensors for environmental monitoring," *Anal. Methods*, vol. 9, no. 1, pp. 55–65, 2017, doi: 10.1039/C6AY02949C.

[147] S. M. Borisov, G. Nuss, W. Haas, R. Saf, M. Schmuck, and I. Klimant, "New NIR-emitting complexes of platinum(II) and palladium(II) with fluorinated benzoporphyrins," *Journal of Photochemistry and Photobiology A: Chemistry*, vol. 201, 2-3, pp. 128–135, 2009, doi: 10.1016/j.jphotochem.2008.10.003.

[148] PyroScience GmbH, *OXCAPG-UHS-SUB: Ultra High-Speed Oxygen Sensor*. Datasheet. [Online]. Available: https://www.pyroscience.com/en/products/all-sensors/oxcapg-uhs-sub#Downloads (accessed: Nov. 24 2020).

[149] V. R. Martin Tscherner, "Optochemical sensor," WO2013181679A1, Dec 12, 2013.

[150] PyroScience GmbH, *OXR50-UHS: Retractable Fiber Oxygen Microsensor*. Datasheet. [Online]. Available: https://www.pyroscience.com/en/products/all-sensors/oxr50-uhs#Downloads (accessed: Nov. 24 2020).

[151] PyroScience GmbH, *OXROB10: Robust Oxygen Probe*. Datasheet. [Online]. Available: https://www.pyroscience.com/en/products/all-sensors/oxrob10#Downloads (accessed: Nov. 24 2020).

[152] Unisense, *O2 MicroOptodes*. Datasheet. [Online]. Available: https://www.unisense.com/MicroOptode (accessed: Nov. 24 2020).

[153] S. O. McDonnell and D. F. O'Shea, "Near-infrared sensing properties of dimethlyamino-substituted BF2-azadipyrromethenes," *Organic letters*, vol. 8, no. 16, pp. 3493–3496, 2006, doi: 10.1021/ol061171x.

[154] J. Murtagh, D. O. Frimannsson, and D. F. O'Shea, "Azide conjugatable and pH responsive near-infrared fluorescent imaging probes," *Organic letters*, vol. 11, no. 23, pp. 5386–5389, 2009, doi: 10.1021/ol902140v.

[155] PyroScience GmbH, *Sensor Spots: For measurements in closed containers*. Datasheet. [Online]. Available: https://www.pyroscience.com/en/products/oxygen/contactless-sensors (accessed: Nov. 24 2020).

[156] PreSens Precision Sensing GmbH, *Microx TX3: Micro-fiber Optic Oxygen Transmitter*. [Online]. Available: https://www.presens.de/products/detail/microx-tx3 (accessed: Nov. 24 2020).

[157] MIchael J. Morris, Mahoumd R. Shahriari, "Enhanced scattering membranes for improved sensitivity and signal-to-noise of optical chemical sensors, fiber optic oxygen sensor for real time respiration monitoring utilizing same, and method of using sensor," US20030068827A1, Apr 10, 2003.

[158] Ocean Insight, Inc., *NeoFox: Phase Fluorometer*. [Online]. Available: https://www.oceaninsight.com/globalassets/catalog-blocks-and-images/manuals--instruction-old-logo/sensors/neofox-operation-manual.pdf (accessed: Nov. 24 2020).

[159] Ocean Insight, Inc., *Oxygen Bifurcated Fibers*. [Online]. Available: https://www.oceaninsight.com/products/sampling-accessories/sensors/oxygen/oxygen-bifurcated-fibers/ (accessed: Nov. 24 2020).

[160] PyroScience GmbH, *FDO2: Optical Oxygen Gas Sensor*. Datasheet. [Online]. Available: https://www.pyroscience.com/en/products/all-meters/fdo2#downloads (accessed: Nov. 24 2020).

[161] Dr. Roland Thar, Dr. Jan Fischer, "Vorrichtung zur Ermittlung der Konzentration eines Analyten in einem gasförmigen Medium," DE102016114918, Nov 2, 2017.

[162] PyroScience GmbH, *AquapHOx: Underwater Oxygen Sensors*. Datasheet. [Online]. Available: https://www.pyroscience.com/en/applications/applications/underwater-solution (accessed: Nov. 24 2020).

[163] PyroScience GmbH, *FireSting pro: Optical pH & Oxygen & Temp Meter*. Datasheet. [Online]. Available: https://www.pyroscience.com/en/products/all-meters/fspro-1#downloads (accessed: Nov. 24 2020).

[164] PreSens Precision Sensing GmbH, *OXY-1 ST: Compact Oxygen Transmitter*. [Online]. Available: https://www.presens.de/products/detail/oxy-1-st (accessed: Nov. 24 2020).

[165] J. Ehgartner *et al.,* "Online analysis of oxygen inside silicon-glass microreactors with integrated optical sensors," *Sensors and Actuators B: Chemical*, vol. 228, pp. 748–757, 2016, doi: 10.1016/j.snb.2016.01.050.

[166] M. Larsen *et al.,* "In situ quantification of ultra‐low O 2 concentrations in oxygen minimum zones: Application of novel optodes," *Limnol. Oceanogr. Methods*, vol. 14, no. 12, pp. 784–800, 2016, doi: 10.1002/lom3.10126.

[167] PyroScience GmbH, *PICO2: Ultra-Compact Oxygen Meter*. Datasheet. [Online]. Available: https://www.pyroscience.com/en/products/all-meters/pico2#downloads (accessed: Nov. 24 2020).

[168] PreSens Precision Sensing GmbH, *OXYLogger: Wireless O2 Measurement Device for Product Monitoring*. [Online]. Available: https://www.presens.de/products/detail/oxylogger (accessed: Nov. 24 2020).

[169] PreSens Precision Sensing GmbH, *PM-PSt8: Oxygen Microsensor*. [Online]. Available: https://www.presens.de/products/detail/profiling-oxygen-microsensor-pm-pst8 (accessed: Nov. 24 2020).

[170] PreSens Precision Sensing GmbH, *OIM-PSt6: Oxygen Probe for In-Line Measurement*. [Online]. Available: https://www.presens.de/products/detail/oxygen-probe-for-in-line-measurement-oim-pst6 (accessed: Nov. 24 2020).

[171] Unisense, *Opto-430 Fast: O2 MicroOptode*. Datasheet. [Online]. Available: https://www.unisense.com/files/PDF/Produktark/MicroOptode%20Portfolio.pdf (accessed: Nov. 24 2020).

[172] World Precision Instruments, Inc., *BioOxy Optical Oxygen Sensors: Oxygen Microsensors.* [Online]. Available: https://www.wpiinc.com/var-biooxy-biooxy-optical-oxygen-sensor (accessed: Nov. 24 2020).

[173] PyroScience GmbH, *PHCAP-PK7-SUB: pH Sensor Cap for Underwater Devices*. Datasheet. [Online]. Available: https://www.pyroscience.com/en/products/all-sensors/phcap-pk7-sub#Downloads (accessed: Nov. 24 2020).

[174] PreSens Precision Sensing GmbH, *PM-HP5: pH Microsensor.* [Online]. Available: https://www.presens.de/products/detail/profiling-ph-microsensor-pm-hp5 (accessed: Nov. 24 2020).

[175] PreSens Precision Sensing GmbH, *FTC-SU-HP5-US: pH Flow-Through Cell.* [Online]. Available: https://www.presens.de/products/detail/single-use-ph-flow-through-cell-ftc-su-hp5-us (accessed: Nov. 24 2020).

[176] PreSens Precision Sensing GmbH, *SP-HP5-SA: Self-adhesive pH Sensor Spot.* [Online]. Available: https://www.presens.de/products/detail/self-adhesive-ph-sensor-spot-sp-hp5-sa (accessed: Nov. 24 2020).

[177] World Precision Instruments, Inc., *pH Sensor System.* [Online]. Available: https://www.wpiinc.com/applications/spectroscopy/optical-sensing-systems (accessed: Nov. 24 2020).

[178] PreSens Precision Sensing GmbH, *PM-CDM1: pCO2 Microsensor (Prototype).* [Online]. Available: https://www.presens.de/products/detail/profiling-pco2-microsensor-pm-cdm1-prototype (accessed: Nov. 24 2020).

[179] PyroScience GmbH, *TPR430: Retractable Fiber Temperature Minisensor*. Datasheet. [Online]. Available: https://www.pyroscience.com/en/products/all-sensors/tpr430#Downloads (accessed: Nov. 24 2020).

[180] PreSens Precision Sensing GmbH, *OXYPro: Wide Range Oxygen Probe.* [Online]. Available: https://www.presens.de/products/detail/wide-range-oxygen-probe-oxypro-wr (accessed: Nov. 24 2020).

[181] Unisense, *FOM Deep: Field Opto UniAmp*. Datasheet. [Online]. Available: https://www.unisense.com/files/PDF/Produktark/Field%20Opto%20UniAmp.pdf (accessed: Nov. 24 2020).

[182] PreSens Precision Sensing GmbH, *pH-1 SMA HP5: Compact Fiber Optic pH Meter.* [Online]. Available: https://www.presens.de/products/detail/ph-1-sma-hp5 (accessed: Nov. 24 2020).